Annu. Rev. Earth Planet. Sci. 2000. 28:509–37
Copyright © 2000 by Annual Reviews. All rights reserved

HETEROGENEITY OF THE LOWERMOST MANTLE

Edward J. Garnero
Department of Geology, Box 871404, Arizona State University, Tempe, Arizona, 85287–1404; e-mail: garnero@asu.edu

Key Words seismic heterogeneity, core-mantle boundary, D″, ultra-low velocity zone, mantle structure

■ **Abstract** Strong heterogeneity at a variety of scale lengths has been imaged in the lowermost mantle using different forward and inverse methods. Coherent patterns in differential travel times of waves that sample the base of the mantle—such as diffracted shear waves (Sdiff) and compressional waves (Pdiff)—are readily apparent, and are compared with results from tomographic studies. Travel time and waveform modeling studies have demonstrated the presence of intense lateral variations in a variety of mapped features, such as a regionally detected high velocity D″ layer, ultra-low velocity zones, D″ anisotropy, strong scattering and heterogeneity. Such short-wavelength variations currently preclude confident mapping of D″ structure at smaller scales. Issues of seismic resolution and uncertainties are emphasized here, as well as the limitations of one-dimensional modeling/averaging in highly heterogeneous environments.

INTRODUCTION

Earth's two most significant boundary layers, the surface and the core-mantle boundary (CMB), are characterized as having the richest thermal, chemical, and dynamic behavior of the planet. The focus of this paper is the deeper of the two layers—specifically, the mantle side of the CMB. The remote sensing tool of seismology is used for this study, because it is the most effective probe for mapping the deepest mantle. In the past several years, a host of seismic studies have focused on various aspects of the lowermost mantle, along with its possible relationship to whole-mantle processes.

It has long been known that the properties of the lowermost part of the mantle are unique compared to those of the rest of the lower mantle. Bullen (1949) dubbed this region the D″ region, and noted the presence of anomalous velocity gradients as compared to the rest of the overlying lower mantle. One-dimensional seismic reference Earth models, such as the commonly cited models PREM (Dziewonski & Anderson 1981) and *iasp91* (Kennett & Engdahl 1991), also contain a change in velocity gradient in the bottom 150 km or so of the mantle. This is most commonly attributed to a thermal boundary layer at the base of the mantle resulting from an expected large temperature drop across D″—up to 1500° C (e.g. see Williams 1998). However, as we will discuss, the possibility of a chemically distinct component to D″ has been gaining popularity in recent years. In fact, recent consideration of aspherical lower mantle structure (van der Hilst & Kárason 1999), along with dynamical calculations (Kellogg et al 1999), has resulted in a model where a compositionally distinct layer in the lower half of the lower mantle exists, with a highly variable surface from 1600 km depth to the core mantle boundary.

This paper emphasizes the bottom 50–300 km of the mantle. We wish to better understand how well (or poorly) various proposed features are resolved. This is a difficult task, especially in view of the strong possibility that structure and dynamics in the lowermost mantle are coupled with that above it. With the pervasiveness of lateral and radial smearing, poor path coverage, noisy data, and limited wave propagation tools (to name a few) in lower mantle seismic studies, the urge to dismiss even the most conservative conclusions is present. Seismological studies have yielded evidence for a lowermost mantle structure with many different scale lengths and amplitudes. Although it is desirable to reconcile seemingly disparate results, this is not possible in some cases because of incomplete information (data, coverage, etc). The approach here is to present raw data and resulting models, while considering scale length of heterogeneity and resolution along the way. Several recent papers have summarized many aspects of deep mantle study, so this is not intended as an exhaustive review of overall lower mantle features; rather, we attempt to consider the studies that relate most directly to the lowermost mantle structure, heterogeneity, and dynamics. For recent reviews of deep mantle structure, see Loper & Lay (1995), Weber et al (1996), Lay et al (1998a,b), Wysession et al (1998), and Garnero et al (1998).

A decade and a half ago, long wavelength trends in lower mantle heterogeneity were identified (e.g. Dziewonski 1984). Subsequent work emphasized the importance of the lower mantle system and how it relates to whole-mantle circulation: Thermal/density anomalies in the deep mantle drive viscous flow, resulting in topography at the CMB as well as the Earth's surface (e.g. Hager et al 1985). These studies and others demonstrated the incredible utility of the inversion method applied to deep Earth structure. Dozens of studies since the mid-1980s have reconfirmed the dominant long wavelength patterns in the lowermost mantle: a degree 2 low-velocity pattern with lows beneath the Pacific and Africa, and a high-velocity ring surrounding these lows, i.e. the circum-Pacific (e.g. Tanimoto 1990, Fukao 1992, Su et al 1994, Li & Romanowicz 1996, Masters et al 1996, Ritzwoller & Lavely 1995, Grand et al 1997, van der Hilst et al 1997, Kennett et al 1998, Vasco & Johnson 1998).

Forward modeling has complemented tomographic studies, providing details of structural features as well as smaller-scale patterns of heterogeneity. These studies have most commonly used differential time information between two phases that travel similar upper mantle paths. Waveform modeling of seismic phases arriving close together (raw data as well as data stacks) and amplitude ratios of neighboring phases have also been successfully employed to image deep Earth structure, such as the D″ discontinuity. Because most tomographic inversions rely on differential travel time data sets of deep Earth phases for improved lower mantle resolution, we survey these particular data sets.

In past studies, researchers have carefully measured their own differential travel times, as well as used those from the large data set of the International Seismological Centre (ISC). Although the ISC travel times have been critiqued because of uncertainties in travel time picking methods, a careful reprocessing of the data (Engdahl et al 1998) has resulted in global images of lower mantle structure from ISC P times that look remarkably similar to those from non-ISC S times (e.g. see Grand et al 1997; van der Hilst et al 1997, 1998).

Careful measurements and analyses of differential times sensitive to lower mantle structure are routine now in regional studies, and have been for more than 25 years (Mitchell & Helmberger 1973). In the next section we discuss some of the regional studies along with large global differential-time data sets. A section on long wavelength heterogeneity follows that one, and then one on short wavelength heterogeneity. The separation of some topics in terms of small or large wavelengths is somewhat artificial. The hope here is to give a general sense of the gross features in the long wavelength section (generally provided from tomographic inversion studies), and of the more detailed structural features in the small wavelength section (which are more commonly from forward modeling studies). Here we adopt ‘‘small’’ and ‘‘large’’ wavelengths to roughly correspond to less and greater than approximately 500–1000 km, respectively. Table 1 lists some candidate lower mantle features and proposed dimensions. While modeling uncertainties are often large, it is clear that many features have both long- and short-scale attributes. In sections that follow, we present differential travel time data sets, followed by tomographically derived aspherical D″ structures.

TABLE 1 Lower mantle features and possible attributes

Feature	Horiz l	Vertical l	Method	Seismic phase	Possible source of trade-off
Plume/upwelling	100–3000*x*	500–2890	T,FM	Many[a]	Mantle heterogeneity
ULVZ	100–1000*x*	5–50	FM	SPdKS, PcP, ScP	Fuzzy CMB, CRZ
D″ high velocities	500–5000*x*	150–350	T,FM	Many[b]	D″ thickness vs. dV redux
D″ anisotropy	500–5000*x*	50–300	FM	ScS, Sdiff	Volumetric D″ heterogeneity
Scatterers	5–50	5–50	FM	PKP, Pdiff	Volumetric vs. topographic

T, tomography; FM, forward modeling; *x*, maximum or minimum scale not well resolved/understood due to coverage limitations

[a]Normal modes, mantle waves, and body waves (e.g. S, Sdiff, ScS, SKS)

[b]Normal modes, mantle waves, and body waves (e.g. S, P, Sd, Pd, ScS, PcP, Scd)

DIFFERENTIAL TRAVEL TIMES

Ray Path Geometries

Differential travel times of deep mantle phases can be very useful for lower mantle study, because source error effects and contamination due to unmapped mantle heterogeneity can be minimized. Differential travel times have been the focus of many recent studies (e.g. Valenzuela & Wysession 1998, Bréger & Romanowicz 1998, Russell et al 1999). Seismic phase pairs with similar mantle paths are usually chosen. Figure 1 (color insert) displays ray path geometries of phases previously used for inference on mantle structure. Also displayed is information regarding geometry of the D″ path, such as path length in D″ and path separations. For example, Figure 1*a* shows the paths of S and ScS. At distances less than ~70°, S waves have turning depths of 1000 km or more above the CMB. Thus, at these distances, one must be careful if interpreting anomalies as solely due to D″ structure, because the S and ScS paths are quite different. At greater distances, however, S bottoms more deeply, eventually becoming asymptotic to ScS, and ScS path lengths in D″ increase significantly (Figure 1*a*). Woodward & Masters (1991) presented a large global data set of ScS-S times, which revealed long wavelength patterns in lower mantle heterogeneity. This data set has been used in several subsequent tomographic inversion studies (e.g. Su et al 1994). Recent regional and global studies have illustrated the utility of these waves (e.g. Wysession et al 1994, Castle et al 2000).

Referencing diffracted waves to core wave counterparts, such as S(Sdiff)-SKS (Figure 1*b*) and Pdiff-PKP (Figure 1*c*), produces sensitive indicators of D″ heterogeneity. Because of the long diffracted wavepath in D″ relative to the short path of the reference core phase, this pair is thought to effectively provide information on D″ heterogeneity. However, the separation between Sdiff and SKS (as well as Pdiff and PKP) upon entry to D″ is typically >1000 km. Therefore, the presence of any lower mantle heterogeneity extending out of D″, sampled by either the diffracted or core wave, will bias models that assume anomalies are solely accrued in D″. The diffracted path length in D″ is quite large (Figure 1*b,c*), so any short-scale variations will be smoothed out in studies using these difference times. Nonetheless, important intermediate- to long-wavelength variations can be mapped with these data (Wysession 1996a, Kuo & Wu 1997, Kuo et al 2000), along with regional reference structure information (Ritsema et al 1997, Kuo 2000).

A probe of short-scale P (and indirectly S) structure at the very base of the mantle is SPdKS referenced to SKS (Figure 1*d*). Mantle paths of these phases are nearly identical, except where the P diffracted segment in SPdKS occurs. At the smallest distances for SPdKS (108–110 deg), the P diffraction arcs are quite small (Figure 1*d*), providing a spot sample of P structure (see Garnero et al 1998). However, a large uncertainty comes from not knowing a priori whether the anomalous structure is at the source or receiver side of the path. This uncertainty holds for the phases shown in Figure 1*d*–*f*.

The differential times of the higher multiple SKS phases with underside CMB reflections, called SmKS, can also provide constraints on lower mantle shear structure (e.g. Sylvander & Souriau 1996a). Separations between these phases upon entering the CMB are quite small, especially for the higher multiples (Figure 1*e*). The higher multiples are extremely sensitive to lateral gradients in D″ (Garnero & Helmberger 1995a), because the pair of phases can be collectively perturbed.

More recently, the PKP core phases have received attention for the information they provide on D″ heterogeneity (Figure 1*f*). Studies have interpreted precursors to PKP in terms of scattering (e.g. Hedlin et al 1997, Vidale & Hedlin 1998, Wen & Helmberger 1998, Hedlin & Shearer 2000) as well as heterogeneity near the CMB (e.g. Poupinet et al 1993, Song & Helmberger 1997, Bréger et al 2000). As with the higher multiple SmKS data, PKP(BC-DF) enter the CMB separated by only small distances. For this reason, it is commonly thought that large BC-DF residuals cannot be due to D″ structure, since heterogeneity must be smaller-scale than the separation between BC and DF (200–600 km, Figure 1*f*). However, strong lateral gradients can perturb ray parameters of the pair to be mapped into a different equivalent ray parameter (i.e. distance), exactly as with the SmKS higher multiples. Some anomalies in BC-DF that correlate with edges of ultra-low velocity zone structure have been noted (Bowers et al 2000). Similar studies to SmKS involve the multiple underside CMB reflections for the PKP data (not shown in Figure 1), e.g. PKKP (Earle & Shearer 1997, 1998; Shearer et al 1998), which have recently been used for the study of scattering using precursors.

Differential Travel Time Patterns

In this section, we show differential travel times of several different phases projected onto a map. The first set of phases considered are diffracted S and P referenced to SKS and PKP, respectively (Figure 2, color insert). Past studies of diffracted phases referenced to core phases have provided detailed information regarding patterns of deep mantle lateral heterogeneity (e.g. Garnero & Helmberger 1993, Wysession et al 1995, Wysession 1996c, Kuo & Wu 1997, Ritsema et al 1997, Vinnik et al 1998, Berger & Romanowicz 1998). These times are routinely used in whole-mantle tomographic studies (e.g. Liu & Dziewonski 1994, 1998; Grand 1994; Grand et al 1997). The high-velocity ring around the Pacific is readily seen in the raw times smoothed by a 5° Gaussian cap (Figure 2), along with the degree 2 low velocities underlying the Pacific and Africa. It is important to keep in mind that averaging in the manner of Figure 2*c* destroys possible depth trends in the residuals, which may certainly be inappropriate, since anomalies probably vary differently with depth from region to region (especially when the smallest wavelengths are considered). The collection of approximately 1500 S_{diff}-SKS times are from the study of Kuo et al (2000), and were also used by Castle et al (2000); the 532 PKP-P_{diff} times are from Wysession (1996c).

The differential time between ScS and S provides a powerful probe of lower mantle structure because it is very sensitive to deep-mantle lateral variations—without the extent of lateral averaging in diffracted waves, since D″ path lengths are typically much shorter for ScS (see Figure 1). A possible drawback for ScS-S is the potential contamination from the structure outside of (above) D″, owing to S bottoming depths far above D″. When plotted and smoothed, however, the ScS-S residuals show similar long wavelength trends to those of Sdiff-SKS (Figure 3, color insert). The ScS-S data show the shorter wavelength variations (as expected) than are seen in Sdiff-SKS. These 4864 ScS-S times are from Castle et al (2000), who assembled times from the studies of Woodward & Masters (1991) and Winchester & Creager (1997).

The differential times of core phases can also provide valuable information for lowermost mantle structure. Figure 4 (color insert) displays travel time residuals of SKKS-SKS and PKPAB-DF. These phase pairs can provide information on short, intermediate, and long wavelength heterogeneity, if the path coverage is dense enough. Sylvander & Souriau (1996a,b) used these differential times in inversions for lowermost mantle structure. A potential large uncertainty in using differential times of core phases concerns the source or receiver side of path ambiguity. Only dense crossing ray path coverage can adequately reduce this uncertainty. This problem seems apparent in Figure 4—variations are small-scale, and are not highly correlated with the ScS-S or Sdiff-SKS maps of Figures 2 and 3. This may result either from the source-receiver ambiguity or from the fact that these differential times are sensitive to strong smaller-wavelength heterogeneity.

The path lengths of SmKS waves in the outer core are a significant portion of the total wavepaths. The data set of SKKS-SKS (from Sylvander & Souriau 1996a, and Garnero & Helmberger 1995b) is biased with large SKKS-SKS separations. This may result from the radial profile of outermost core velocities being too high in the PREM reference model (as has been proposed in several studies of SmKS, e.g. Souriau & Poupinet 1993, Lay & Young 1990, Garnero et al 1993). For this reason, the mean has been subtracted from the SKKS-SKS times displayed in Figure 4. Also displayed are PKPAB-DF times in the right column. As with the SKKS-SKS times, the AB-DF residuals display short wavelength variations that do not readily correlate with the long wavelength patterns of Pdiff-PKP (in Figure 2). No mean has been subtracted from the PKP times in Figure 4. Both AB and DF cross the outermost core steeply, and should be similarly affected, whereas the SKKS crosses the outermost core 4 times, compared to twice for SKS.

We have thus shown trends of some of the differential travel time data sets commonly used in forward modeling efforts and also tomographic inversion. Figures 2, 3, and 4 show data sets that were carefully measured by hand. One could also compare these to the same with ISC data, which would ostensibly compare well at the longer wavelengths. In the next section, we discuss long- and short-wavelength heterogeneity in the lowermost mantle, referring to the travel time figures as well as maps from tomographic inversion.

LONG WAVELENGTH HETEROGENEITY

In this section, large-scale patterns in lower mantle heterogeneities are discussed. Here, large-scale is meant to imply patterns with dominant wavelengths greater than ~1000 km. Inference for large-scale heterogeneity was already seen from patterns in differential times of diffracted waves (Figure 2). Now we compare this to results from whole-mantle tomographic inversion of global data sets. The dominance of degree 2 heterogeneity has been noted in past efforts (e.g. Su & Dziewonski 1991, 1992). Significant small- to intermediate-scale features have been put forth in regional forward modeling efforts (Weber 1993, Lay et al 1997), and are likely superimposed onto the long wavelength patterns. Figure 5 (color insert) presents D″ aspherical structure for four models of shear perturbations (Figure 5*a-d*), and two models of compressional perturbations (Figure 5*e,f*). The shear models of Grand (1994) (and Grand et al 1997), Li & Romanowicz (1996), Liu & Dziewonski (1994, 1998), and Masters et al (1996) and compressional models of van der Hilst & Kárason (1999) and Bijwaard & Spakman (1999) are shown. The choice of models is somewhat arbitrary, but these were chosen to represent models frequently cited in deep Earth studies. The long wavelength trends in lowermost mantle structure have been known for quite some time (e.g. Dziewonski 1984). In many other significant contributions over the years, large-scale, lower-mantle heterogeneity has been characterized in tomographic inversion studies using a wide variety of data sets, from normal modes to travel times. For examples of this, see studies or reviews by Tanimoto (1990), Fukao (1992), Ritzwoller & Lavely (1995), Dziewonski (1996), Vasco & Johnson (1998).

The long-wavelength character of the different maps in Figure 5 is quite consistent. The details of the shapes of features, as well as amplitudes, are different, but all models show low velocities beneath the Pacific and west Africa, and high velocities under the Americas and Eurasia. As you will see, forward modeling efforts more commonly use these models as starting structures in their modeling procedure.

Although it has long been supposed that thermal-chemical instabilities in the D″ region may be related to the observed strong lateral heterogeneity (e.g. Hansen & Yuen 1988), the origin of the high and low velocities in the maps of Figure 5 have been traditionally interpreted as thermal anomalies. A common hypothesis is that high velocities may be related to slab ‘‘dregs,’’ since the spatial correlation between predicted locations of density anomalies in D″ from slabs falling through the mantle (e.g. Lithgow-Bertelloni & Richards 1998) and seismic high velocities is quite good (see, for example, Lay et al 1998a). More recently, however, alternative hypotheses involving a chemically distinct D″ or a phase change in D″ have gained popularity; these hypotheses are discussed in the next section.

SMALL WAVELENGTH HETEROGENEITY

The past five years have seen advancement in the smallest wavelength of resolution in lower mantle tomography, a result of greater data sampling as well as smaller grid or cell size in the inversion (e.g. Grand 1994, van der Hilst & Kárason 1999, Bijwaard et al 1998). In some cases, inversions are capable of resolving features as small as 1000 km in the deep mantle. In discussions here, small- and intermediate-wavelength structures (i.e. approximately $<$1000 km) are both referred to as small-wavelength. This may cause some confusion—many data types and measurements have spatial patterns of travel time anomalies at short- through long-scale lengths. For example, the now commonly used S_{diff}-SKS data are well suited for medium- to long-scale lower-mantle heterogeneity, especially when averages of large data sets are used. However, a closer look at any given data set exhibits features that point to much smaller-scale lengths of heterogeneity. Figure 6 (color insert) displays S_{diff}-SKS times for a constricted azimuth and region, from the study by Ritsema et al (1997). Figures 6*a* and 6*b* show the path geometry and solution model. The steeply negative gradient was needed to match both the S_{diff}-SKS differential times as well as the S_{diff}(SV)/SKS amplitude ratios. Model M1 best fit the average behavior of the observations. However, as the dashed red lines in Figure 6*c* indicate, a large spread on the data is present, indicating strong small-scale variations about this average structure. The predictions by Liu & Dziewonski (1994) of the aspherical structure match the general character of the data: large scatter and positive residuals at shorter distances and positive slope to the trend at larger distances. However, the scatter and amplitudes in the data are much larger at the greater distances than predictions indicated. This is not surprising, given the smoothing and damping that is typical in whole-mantle inversions, resulting in diminished amplitudes. In fact, recent forward modeling efforts that used inversion results as starting models multiplied amplitudes by up to two, preserving general shapes of anomalies in the inversion maps. For example, Ritsema et al (1998) and Bréger & Romanowicz (1998) increased D″ heterogeneity amplitudes of Li & Romanowicz (1996) and Grand (1994), respectively, to fit differential time data.

Similarly, the data set of ScS-S times shows long- and short-period patterns of residuals (Figure 3). Upon closer scrutiny, coherent smaller-scale patterns are revealed (Figure 7, color insert). Russell et al (1998, 1999) used these patterns to infer flow that feeds the root of the Hawaiian plume. The dense ray path sampling (Figure 7*a*,*b*) exhibits large travel time anomalies to the northeast of the CMB study area (Figure 7*c*). When averaged with a 1.5° Gaussian cap, a coherent pattern is clearly apparent (Figure 7*d*). Russell et al (1998, 1999) also show a clear spatial trend in inferred D″ fast directions from ScS-splitting observations.

A concentrated data sample from this path geometry is displayed in Figure 8 (color insert). Broadband displacement recordings of S and ScS are shown for a Fiji event, along with the prediction for the PREM reference model. A range of ScS delays/advances relative to S (as compared to PREM predictions) range up to 8 seconds (–3 to +5) for this profile; amplitude anomalies are also present. This waveform behavior at distances where S and ScS have quite similar paths is most easily explained by short wavelength heterogeneity (e.g. <500 km) in the lowermost mantle where ScS is isolated from S. The synthetics were computed by the generalized ray method (e.g. Helmberger 1983).

D″ Discontinuity

Since nearly two decades ago, when the earliest suggestions of a high-velocity layer in the lower mantle were made (e.g. Wright & Lyons 1980 for P-waves, Lay & Helmberger 1983 for S waves), dozens of studies have presented an abrupt increase in seismic velocity some 200–300 km above the CMB (for review, see Weber et al 1996, Wysession et al 1998). Arguments have been made for a D″ layer origin of a chemically distinct layer (see Wysession et al 1998), a phase change (e.g. Nataf & Houard 1993, Sidorin & Gurnis 1998, Sidorin et al 1998), and also the result of D″ anisotropy (e.g. Matzel et al 1996, Lay et al 1998b).

High-velocity regions at the base of the mantle, particularly those with fairly large lateral dimensions underlying past/present subduction, have been studied in many forward modeling efforts to quantify the radial velocity structure (see Wysession et al 1998 for review). These structures are often co-located with high-velocity regions in the lower mantle, as depicted from tomographic inversions (e.g. beneath the Caribbean and Alaska). Waveform modeling efforts have favored a first-order discontinuity in seismic velocity some 200–300 km above the CMB.

The sharpness of the top of the D″ layer (i.e. discontinuity) is not particularly well constrained in waveform modeling, and in fact can occur over a 50–75 km transition depth range (e.g. Young & Lay 1987). This is compatible with the results from tomography, which typically employ fairly strong damping and smoothing; thus, the issue of whether the D″ discontinuity is a distinct layer or a ‘‘blob’’ of high velocities seems quite reconciled when the sharpness uncertainties of the two methods (forward and inverse) are considered. If the term layer is used to define a global feature, then it may be inappropriate to call the D″ discontinuity a layer, because it has not been established as a global feature in any way. In fact, its intermittency has been noted in past studies (e.g. Weber 1993, Krüger et al 1995).

Considerable evidence exists for short- to intermediate-scale variations in the raw data, as well as for the mapped structural features in D″ discontinuity studies (e.g. Weber 1993, Kendall & Shearer 1994, Krüger et al 1995, Pointer & Neuberg 1995, Schimmel & Paulssen 1996, Yamada & Nakanishi 1998, Reasoner & Revenaugh 1999). In many D″ studies, resolution is limited owing to lack of crossing ray path coverage. In addition to path coverage limitations, a further difficulty is possible in the focusing/defocusing of energy due to variable velocity gradients and topography; significant mismapping of structural features is possible when using 1-D modeling methods in the presence of strong topographical variations (e.g. Igel & Weber 1996). We further demonstrate this in Figure 9 (color insert), which shows a synthetic experiment of a D″ discontinuity that gradually changes thickness from 300 km to 180 km. The transition is smooth and long-wavelength, occurring laterally over several thousands of km in D″. The structure right above D″ has a smooth transition zone, a model adopted recently by the work of Sidorin & Gurnis (1998). Such a gradient is compatible with a phase transition origin for the D″ high velocity layer. Iso-velocity contours are displayed in Figure 9*a*, along with ray paths to each layer that are summed to give the final response, in this case at 82 degrees (see Helmberger et al 1996a,b). Figure 9*c* displays the synthetics for this structure for three placements of the source, each separated by 500 km. This gives rise to sampling of the dipping surface of the D″ structure in different places, which results in different timing and amplitudes of Scd and ScS relative to S. The bunching of the rays that sample the D″ structure are apparent in Figure 9*a;* resulting waveforms are very sensitive to this behavior, which is of course sensitive to where the gradient structure is sampled.

If these synthetics were interpreted with one-dimensional waveform modeling, large inaccuracies in CMB-to-D″ reflector height as well as D″ properties would result. This, along with modeled D″ thickness variations at a much shorter lateral scale than in Figure 9, e.g. beneath the Arctic (Figure 10, color insert), suggest the extreme complexity and difficulties in accurate determination of D″ discontinuity structure (as well as heterogeneity) at shorter scales.

Lower Mantle Scattering

There is clear evidence for strong heterogeneity at the base of the mantle from small to large wavelength. Scattering studies are typically concerned with short wavelengths, e.g. $<$10 km. The phenomenon of seismic energy reflecting off lowermost mantle heterogeneity has been recently probed in several studies (e.g. Bataille & Lund 1996, Earle & Shearer 1997, Shearer et al 1998, Wen & Helmberger 1998, Vidale & Hedlin 1998, Cormier 1999). The trade-off between CMB topography and lowermost mantle scattering has also been discussed (see Bataille et al 1990). Evidence for scattering throughout the mantle has been proposed as well (Hedlin et al 1997), with arguments for small-scale chemical heterogeneity throughout the mantle. Shearer et al (1998) propose that there is no concentration (at least globally) of scatters at the CMB for the ~8 km scale length (~1% rms amplitudes), which suggests incomplete mantle mixing. Vidale & Hedlin (1998), on the other hand, find at least one zone of concentrated scattering near the CMB in the southwest Pacific, possibly related to partial melt associated with ultra-low velocity zones.

Other studies have addressed reflections of heterogeneity at a slightly larger wavelength, e.g. ~100 km (e.g. Lay & Young 1996, Kaneshima & Helffrich

1998). Scherbaum et al (1997) use a double-beam method to detect scattering heterogeneity of wavelength 10–100 km beneath the Arctic, which may be associated with past subduction there. Earle & Shearer (1998) discuss a probable scattering source to energy associated with PKKP as being due to the deep Earth. Results from the various scattering studies indicate that much work still needs to be done to relate the ultra-small-scale heterogeneity to processes responsible for other proposed deep mantle features.

D″ Anisotropy

As more high-quality data become available from permanent and portable seismic arrays, the deepest mantle can be more effectively and accurately probed. The past five years have seen a host of studies devoted to D″ seismic wave speed anisotropy (see Lay et al 1998). The cause of D″ anisotropy is not certain at present, nor is the nature of anisotropy in the deep mantle well understood—though it may be detected most easily in boundary layers (Montagner 1998). Many questions are posed: Is anisotropy the cause of the D″ reflector used in discontinuity studies (e.g. Matzel et al 1996)? Could former oceanic crust fold and pile in the mantle, forming a layer stack of alternating high- and low-velocity lamellae (e.g. Kendall and Silver 1996)? What is the rheology of the deepest mantle (e.g. Karato 1989, 1998)? What are the elastic constants of probable lowermost mantle material (e.g. Stixrude 1998)? These questions and many others should be addressed simultaneously when considering the possible origin of deep mantle heterogeneity, D″ discontinuity, scattering, and ultra-low velocity zone for the region of study, because these phenomena may be coupled or linked.

Indeed, the possibility of lamellae in the deep mantle has been considered. Weber (1994) discussed high-velocity lamellae as a possible explanation for D″ discontinuity reflections. Thomas et al (1998) show evidence for a low-velocity lamellae in D″ (separated from the CMB), and suggest a partial melt origin. In order for such lamellae to produce shear wave splitting, the lamellae must be thinner than ∼5 km, and must alternate with thin layers of normal mantle over a zone with minimum thickness in depth of ∼75–100 km (Garnero & Lay 1999). It may be difficult to find a dynamically feasible scenario to give rise to the necessary stack of alternating velocities over the large lateral distance needed to produce observed shear wave splits. However, our understanding of lower mantle rheology is admittedly limited at present. We now turn our attention to heterogeneity issues right at, or near, the CMB.

CORE-MANTLE BOUNDARY HETEROGENEITY

In this section, we address some of the heterogeneity issues that exist right at the core-mantle boundary, or that somehow involve the boundary itself. We first turn our attention to evidence for zones containing large velocity reductions, and we follow that with a short discussion on CMB topography; we then discuss the issue of relationship to overlying heterogeneity. These topics are most likely not independent of each other, and are only separated to reflect focus of past studies.

Ultra-low Velocity Zones

Recently, some efforts have turned toward mapping out heterogeneity confined to a thin boundary layer right at the CMB—that is, the ultra-low velocity zone, or ULVZ (see Garnero et al 1998 for summary of recent work). This feature has been characterized by depressed P and S velocities of 10% and greater, occurring in a zone of variable thickness from ~5–50 km. At present, seismic wave CMB Fresnel zones from ULVZ studies cover approximately 44% of the CMB; less than one-third of the investigated regions contain positive identification of a ULVZ (~27% of probed areas or ~12% of the whole globe has ULVZ; Williams et al 1998). The rest of the studied regions are well modeled with standard reference structures, indicating either no boundary layer structure or one too thin for detection.

The origin of the ULVZ may be the partial melt of some lowermost mantle material. P and S velocity reductions of 10% and 30%, respectively, can be achieved with 5%–30% partial melt by volume (5% for film, 30% for tubule inclusions; Williams & Garnero 1996). Thermal anomalies leading to melt can be caused by different means, such as enhanced heat flux from the core or viscous heating (Steinbach & Yuen 1997, 2000). In addition to partial melt, the ULVZ may contain a different chemistry than the bulk lower mantle (Manga & Jeanloz 1996), perhaps as a by-product of chemical reactions between the core and mantle (Knittle & Jeanloz 1989, 1991). If the ULVZ contains material that is significantly more dense than the overlying mantle, important implications arise regarding melt. In considering the definition of seismic velocities, it can be shown that shear modulus reductions (compatible with melting) are precluded when large velocity reductions are accompanied by large density increases (Garnero & Jeanloz 2000). Given the ~74% density increase across the CMB (PREM model), certainly a wide range of densities is permissible for a stable CMB boundary layer. The challenge for future work will include quantifying density increases for iron-enrichment as well as test/explore feasibility of other high-density ULVZ candidate mineralogy.

More detailed study is necessary to determine whether the depressed velocities are confined to the lowermost mantle, the outermost core, a transition between the mantle and core (‘‘fuzzy’’ CMB), or any combination of these possibilities (Garnero & Jeanloz 1999). At present, CMB sharpness is typically constrained to be less than 4 km or so (e.g. Kanamori 1967, Vidale & Benz 1992). Variability in CMB reflectivity has also been reported (Nagumo & McCreery 1992). These studies are compatible with any of the basal layering possibilities.

ULVZ Fresnel zones span large areas on the CMB; details of the structure within these zones, including degree of variability, is only scantly documented at present. This is primarily because of limitations in seismic wavepath coverage, as well as uncertainties owing to modeling trade-offs (Revenaugh & Meyer 1997, Garnero & Helmberger 1998). Some of the trade-offs and uncertainties encountered in ULVZ modeling are presented in Table 2. Strong trade-offs are present, which makes confident estimation of the origin of the ultra-low velocities difficult. However, several key points are certain: (*a*) At least in certain regions, small-scale heterogeneity of order 100 km is necessary to explain many observations (for both SPdKS, e.g. Garnero et al 1998, and PKP precursors, e.g. Wen & Helmberger 1998). Such scales are much smaller than Fresnel zone dimensions. (*b*) ULVZ Fresnel zones are well correlated spatially to surface hot spot locations (Williams et al 1998), leading to the suggestion of a CMB source to mantle plumes that feed hot spots (see also Ribe & de Valpine 1994). (*c*) Lower mantle regions lacking evidence for ULVZ are typically associated with high seismic shear wave speeds in D″. Dynamical calculations predict that dense subducted material will fall to the CMB in these regions (Lithgow-Bertelloni & Richards 1998). This final point suggests that the ULVZ distribution is directly connected to thermal variations at the base of the mantle: ULVZ are lacking where the mantle is being actively cooled by subduction currents, and are present in regions of long-wavelength low velocities—locales that may be characterized by elevated heat flow from the core.

Recent studies involve discussions of intense, small-scale heterogeneity right at the CMB, for example, to explain large PKP precursors (Wen & Helmberger 1998, Vidale & Hedlin 1998). With the proposed origin ascribed to partial melting, the seismic properties of such heterogeneities are not different from those proposed for a basal layer—the only possible difference is the heterogeneity geometry. The PKP data may be explained either by isolated heterogeneity, e.g. pockets of melt of some characteristic wavelength, or by a ULVZ layer with intense topographical or compositional variations. The SPdKS data, on the other hand, require the velocity perturbations to be at the CMB in some continuous

TABLE 2 Trade-offs in modeling a CMB boundary layer (e.g. ULVZ)

Layer property	Trades off with	Reference
Thickness (Z)	ULVZ δVp, δVs, ρ, including δVp:δVs ratio	GH98, HWD98,GJ99
Thickness (Z)	Sharpness of transition from layer to overlying mantle	GH98
Z, δVp, δVs, ρ	Topographic shape of top of layer (e.g. domes)	HWD98
Z, δVp, δVs, ρ	Lateral heterogeneity within the boundary layer	*
Z, δVp, δVs, ρ	Assumption of source- vs. receiver side of SPdKS path	*

δVp, δVs, ρ, VP reduction, VS reduction, and density pertubation, respectively; GH98, Garnero & Helmberger (1998); HWD, Helmberger et al (1998); GJ, Garnero & Jeanloz (2000)
* not a focus of any report as of yet

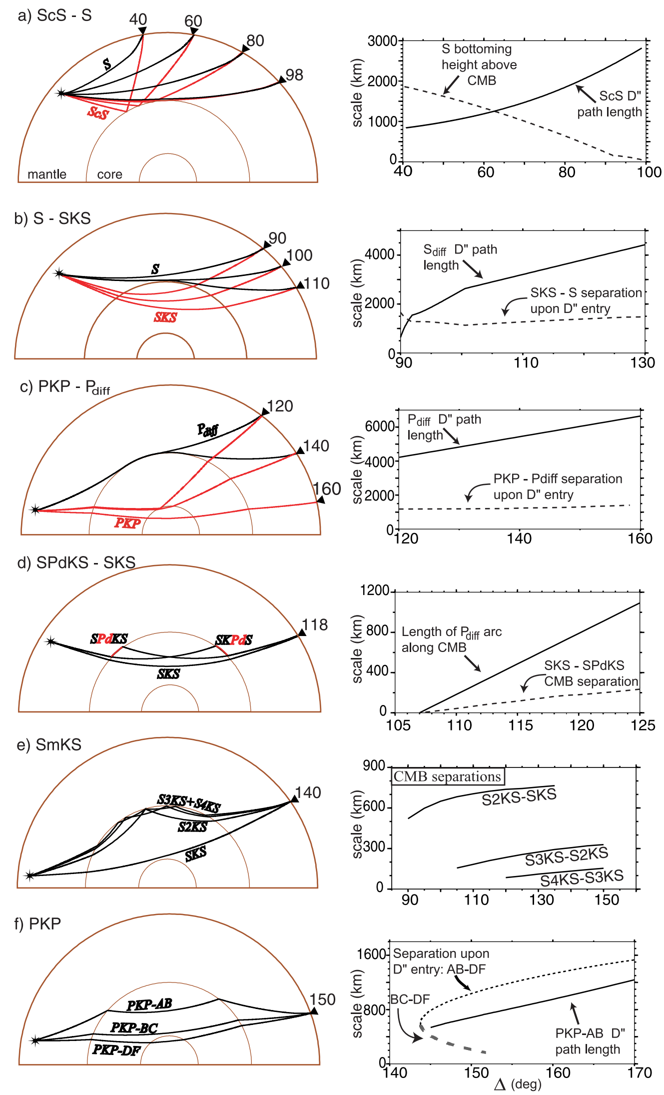

Figure 1 Ray paths and scale lengths of phases used in differential travel time studies. (*a*) ScS-S; (*b*) S_{diff}-SKS; (*c*) P_{diff}-PKP; (*d*) SPdKS-SKS; (*e*) SmKS; and (*f*) PKP. All ray paths and scale lengths are calculated for the PREM model, and D" is assumed to be 300 km thick in the calculations.

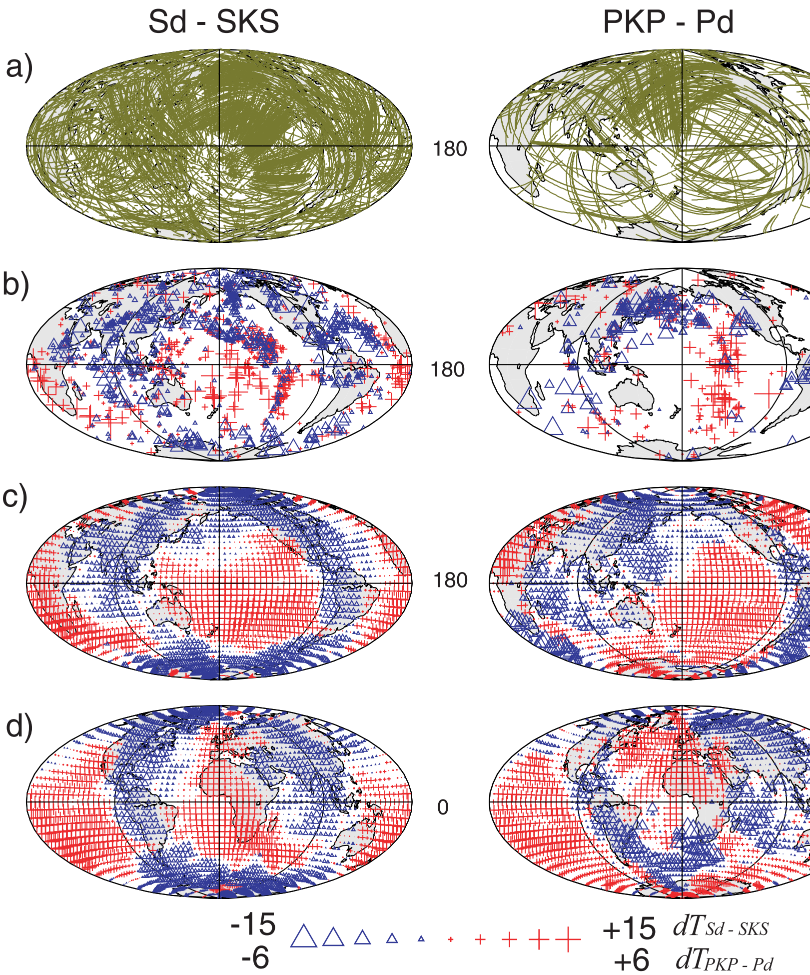

Figure 2 Travel time residuals of diffracted phases referenced to core phases; S_{diff}-SKS (*left column*, from Kuo et al 1999) and P_{diff}-PKP (right column, from Wysession 1996c). (*a*) Coverage for portions of diffracted wave path in a 300 km thick D" layer (1500 data for S, 532 data for P). (*b*) Differential travel time residuals relative to PREM, plotted at path midpoints. (*c*) Residuals assigned to D" paths (in 2° increments) are smoothed via a 5° Gaussian cap average. (*d*) Same as in (*c*) except shown for opposite hemisphere (center of plot longitude shown between columns). Scale at bottom applies to (*b*), (*c*), and (*d*).

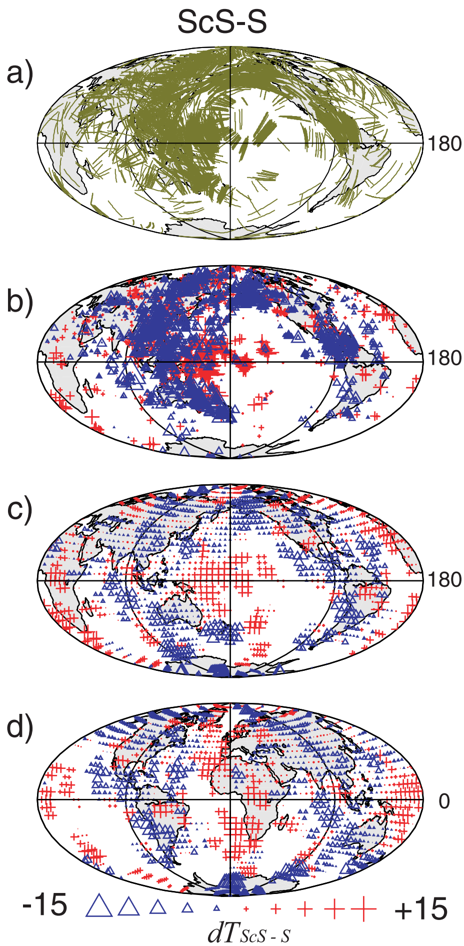

Figure 3 Travel time residuals of ScS waves referenced to direct S. (*a*) Coverage for portions of wave path in a 300 km thick D" layer (4864 times, from Castle et al 1999). (*b*) Differential travel time residuals relative to PREM, plotted at path midpoints. (*c*) Residuals assigned to D" paths (in 2° increments) are smoothed via a 5° Gaussian cap average. (*d*) Same as in (*c*) except shown for opposite hemisphere (center of plot longitude shown on right). Scale at bottom applies to (*b*), (*c*), and (*d*).

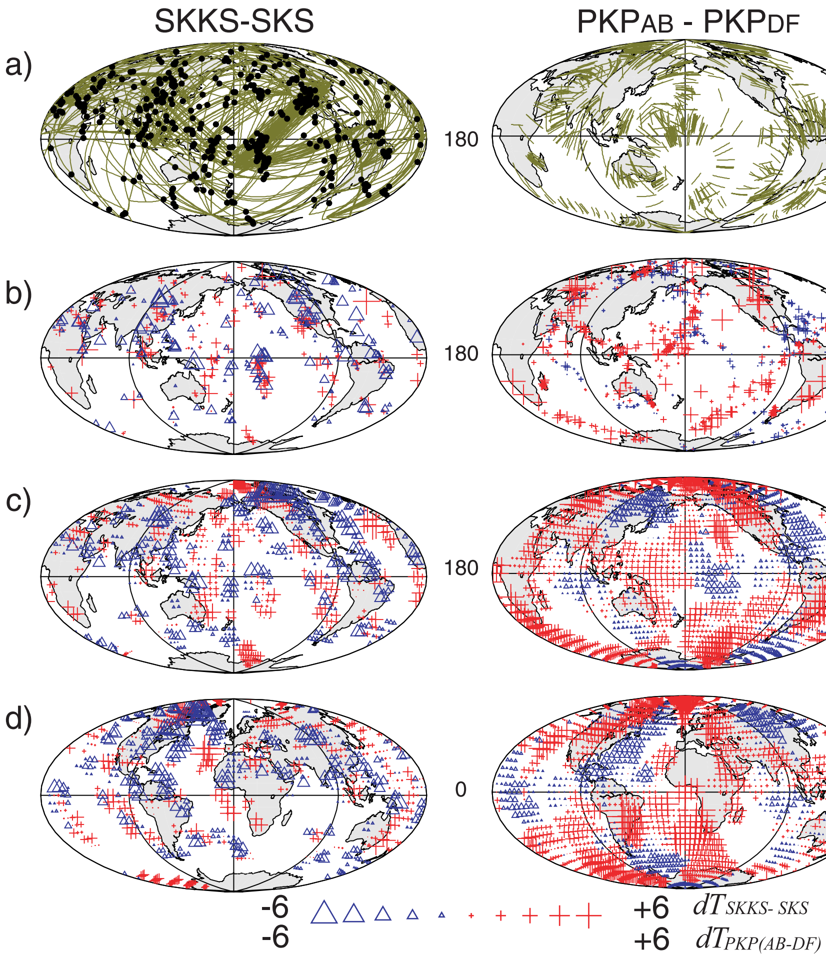

Figure 4 Differential travel time residuals between core phases SKKS and SKS (*left column*, from Sylvander & Souriau 1996a and Garnero & Helmberger 1995b) and PKP_{AB} and PKP_{DF} (*right column*, from Bréger et al 1999) and H Tkalcic, personal communication, 1999). (*a*) For SKKS: complete ray path coverage with dots indicating SKKS CMB crossing locations; for PKP: D" portion of PKP_{AB} paths are shown for a 300 km thick D" layer (234 data for SmKS, 449 data for PKP). (*b*) Differential travel time residuals relative to PREM, plotted at SKKS and PKP_{AB} CMB crossing locations. (*c*) For SKKS: residuals assigned to SKKS CMB crossing location; for PKPAB: residuals assigned to D" paths (in 2° increments), then smoothed with 5° Gaussian cap. (*d*) Same as in (*c*) except shown for opposite hemisphere (center of plot longitude shown between columns). Scale at bottom applies to (*b*), (*c*), and (*d*).

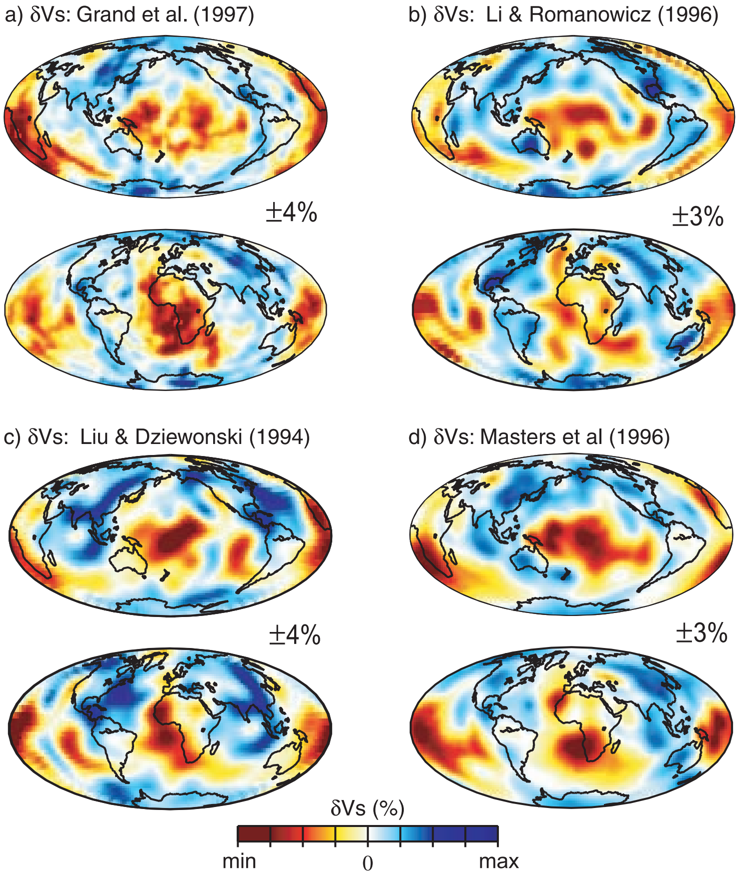

Figure 5 D" heterogeneity as imaged from tomographic inversion studies. Shear perturbations are presented from (*a*) Grand et al 1997, (*b*) Li & Romanowicz 1996, (*c*) Liu & Dziewonski (1994), and (*d*) Masters et al 1996; compressional perturbations are from (*e*) van der Hilst & Kárason 1999 and (f) Bijwaard & Spakman 1999. In all panels, top map is centered on 180° longitude, bottom map on 0° longitude. The maximum and minumum values for the scale bar are shown on the right of each panel. (Figure continues on page 6.)

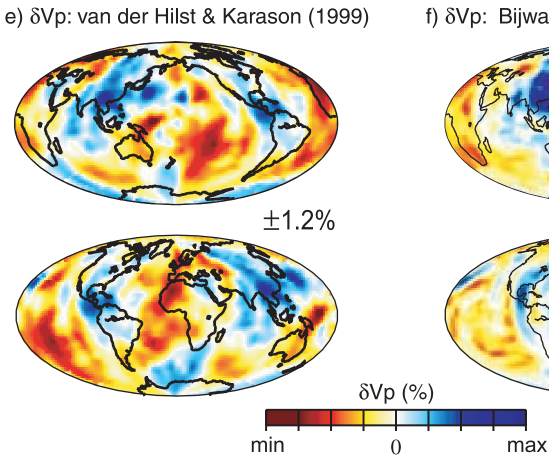
e) δVp: van der Hilst & Karason (1999)
f) δVp: Bijwaard & Spakman (1999)
±1.2%
±1%
δVp (%)
min
0
max

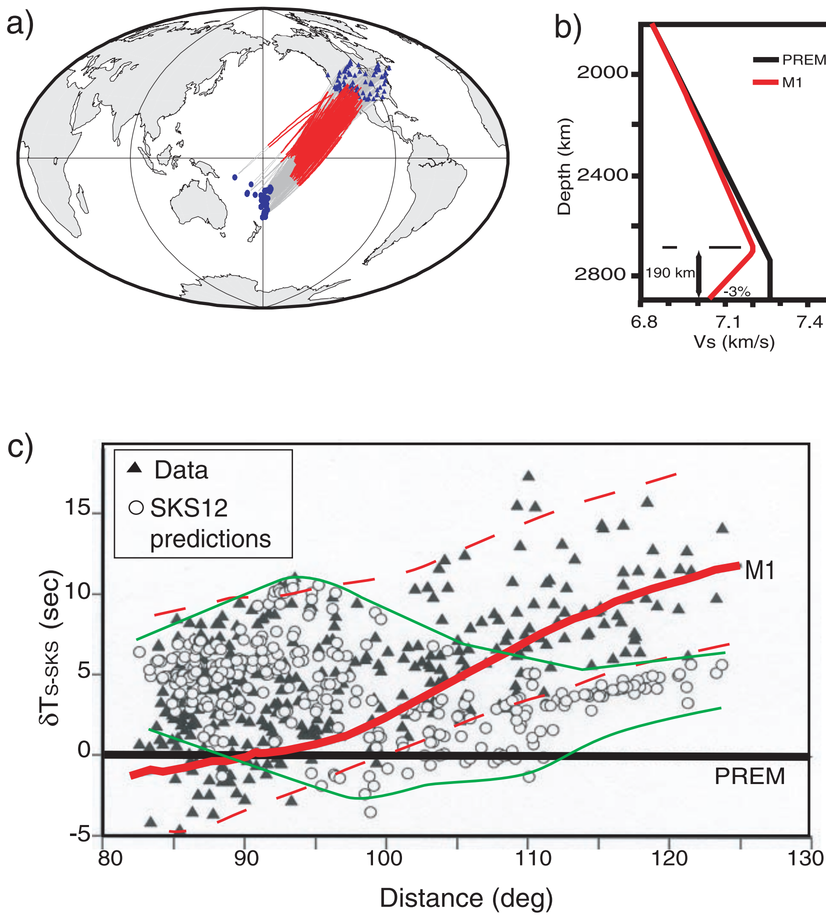

Figure 6 (*a*) Ray paths for southwest Pacific events recorded in North America for S-SKS study of Ritsema et al (1997). D" portions of paths are *red*. (*b*) Solution model that best fits average of amplitude and travel time difference of S and SKS (*red*, M1) compared to PREM (*black*). (*c*) Residual travel time (relative to PREM) observations (*black triangles*) compared to predictions by aspherical structure of model SKS12 of Liu & Dziewonski (1994), the 1-D structure of M1 (*red solid line*). See text for details.

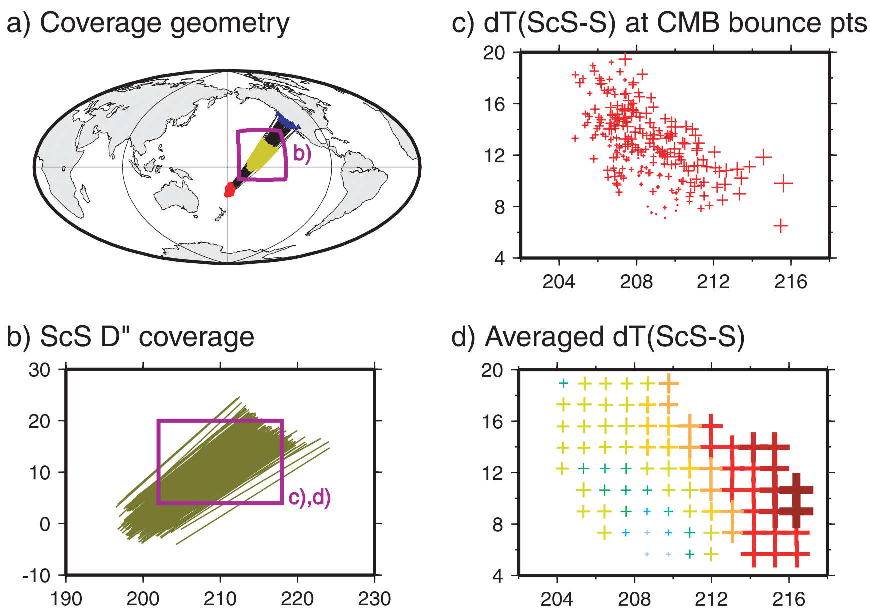

Figure 7 (*a*) ScS-S path geometry of Russell et al (1998, 1999). (*b*) D" portions of ScS paths shown in *green*. Box signifies blow-up region of (*c*) and (*d*). (*c*) Travel time residuals of ScS-S; largest residual amplitudes (*largest* crosses) are ~+7 sec. (*d*) Smoothed residuals (with a 1.5° Gaussian cap). Largest crosses correspond to ~+6 sec, smallest symbols are 0 < dT < 1 sec.

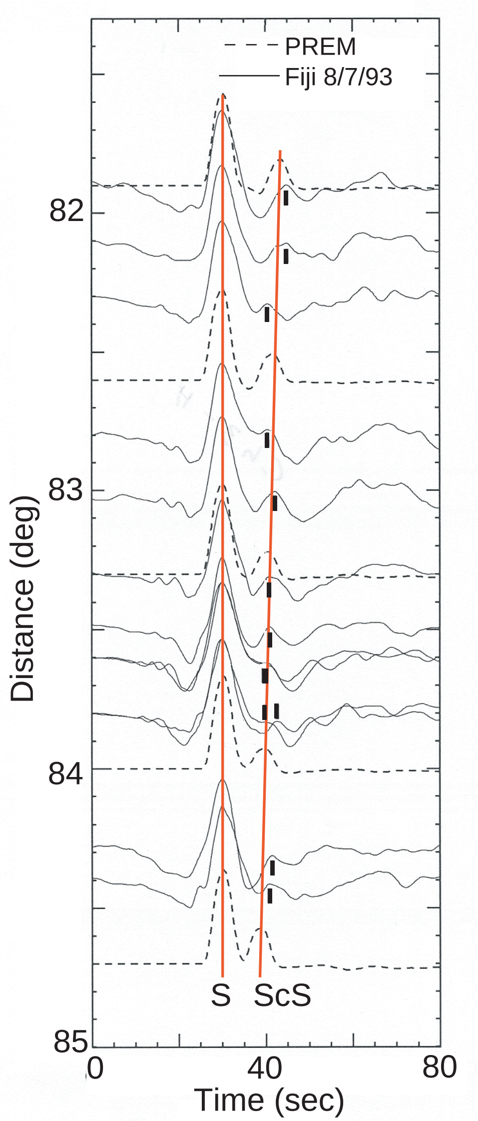

Figure 8 Broadband displacement recordings from the Terrascope and Berkeley arrays of a deep Fiji event. The dominant phases are S and ScS, clearly seen in the data (*solid traces*) and PREM synthetics (*dashed traces*). ScS delays/advances relative to S are indicated by short *black vertical bars*. All traces are normalized in time and amplitude to direct S.

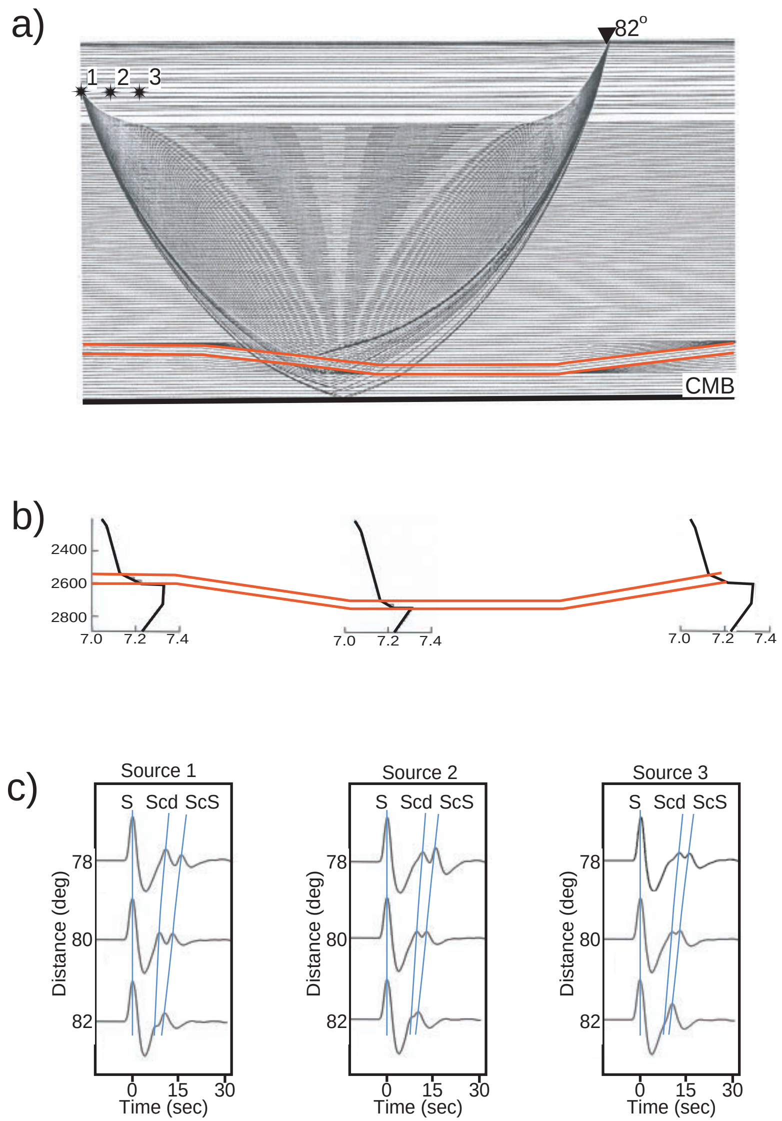

Figure 9 (*a*) Iso-velocity contours (*horizontal lines*) showing lateral changes in D" thickness (*red lines*), along with rays from source location 1 (*leftmost star*) to each layer interface, then to receiver (*triangle*) at 82°. (*b*) Shear wave radial profiles of laterally varying structure in (*a*). (*c*) Tangential component synthetic seismograms produced from 2-D structure of (*a*). Traces are normalized in time and amplitude to the direct S wave. The three profiles correspond to the three source locations in the top panel (*a*).

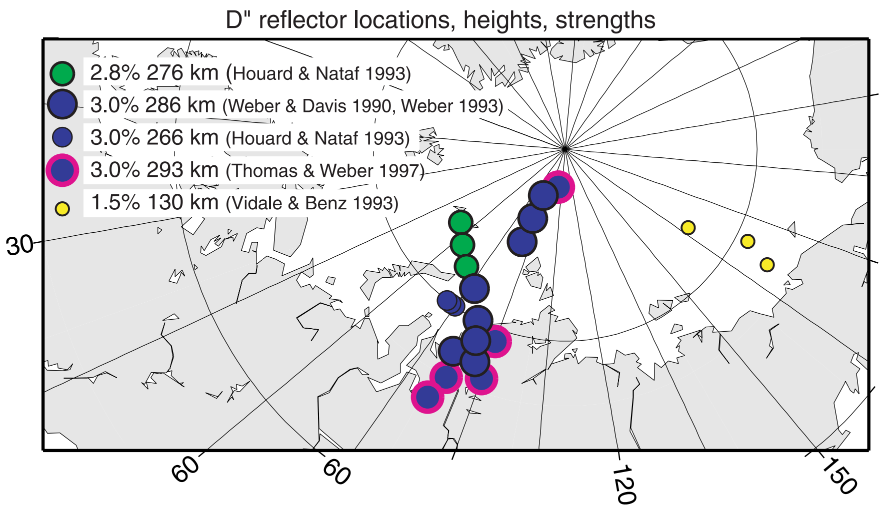

Figure 10 D" reflector depths and velocity increases from forward modeling studies for the region beneath the Arctic. Variations in D" thickness of 25–160 km are suggested. Sources are shown in upper left.

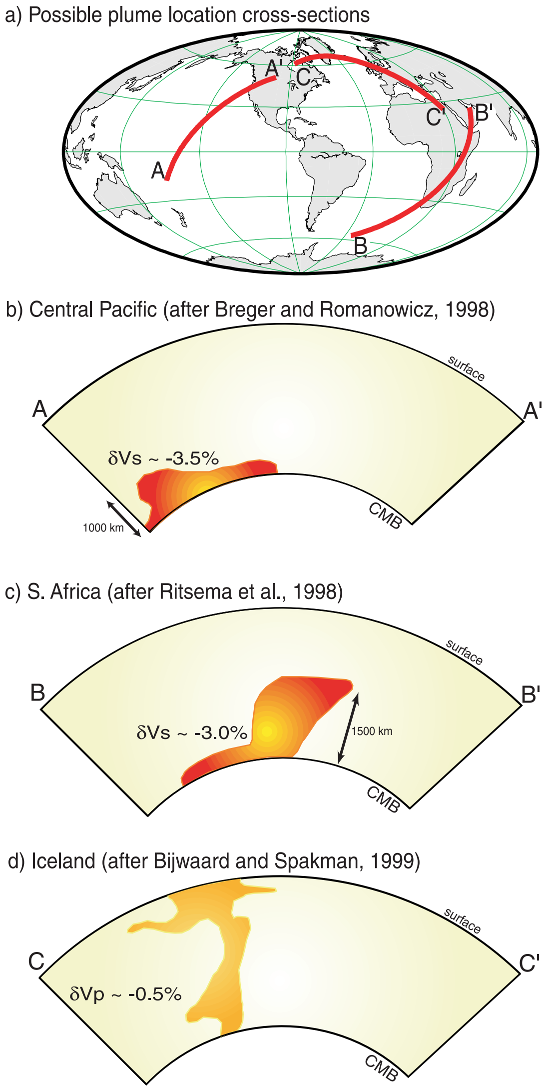

Figure 11 (*a*) Cross-sections for schematic representation of low-velocity structures of (*b*) Ritsema et al (1998) beneath W. Africa, (*c*) Bréger & Romanowicz (1998) beneath the central Pacific, and (*d*) Bijwaard & Spakman (1999) beneath Iceland.

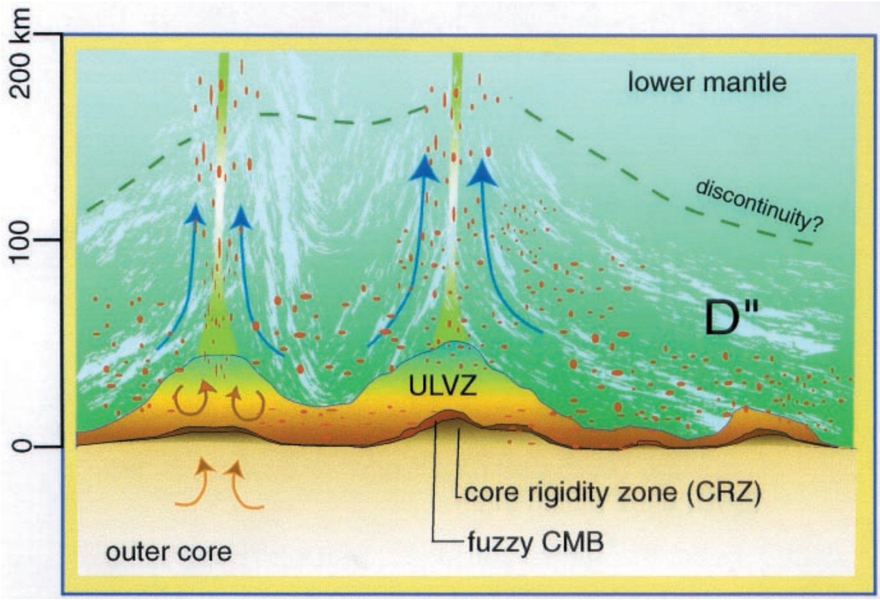

Figure 12 Schematic cartoon of the possible constituent CMB features beneath a warmer than average D" region. This includes an ultra-low velocity zone of partial melt and chemical heterogeneity, a transitional or fuzzyVery go CMB with underside pockets of nonzero rigidity, chemical and melt scatterers throughout D", alignment of crystals, heterogeneity or melt in D" to produce D" anisotropy, and possibly roots of plumes.

fashion so as to generate an observable anomaly. Travel time variations of various P waves, e.g. P_{diff}, PKP, and PcP, have been modeled with high and low velocity heterogeneity ($\pm 10\%$) confined to a zone some 20 km thick at the base of the mantle (e.g. Doornbos & Hilton 1989, Sylvander & Souriau 1996b, Sylvander et al 1997). The ULVZ studies at present differ from this result, in that no zones of ultra-high velocities have been detected or proposed. This probably reflects the fact that ultra-low velocities are easier to detect with SPdKS and ScP or PcP precursors, owing to enhanced amplitudes of delayed signals. Future waveform modeling work should address the possibility of ultra-high velocities at the CMB, as well as causes for these if identified.

Core-Mantle Boundary Topography

Topography or ''roughness'' of the core-mantle boundary is another deep Earth feature that can be investigated at very small wavelength. Past efforts have included discussions of CMB topography at many wavelengths and amplitudes (e.g. Morelli & Dziewonski 1987, Doornbos & Hilton 1989, Rodgers & Wahr 1993, Obayashi & Fukao 1997) using a variety of methods. These studies have little agreement in patterns or amplitudes of topography (see Garcia & Souriau 2000). More recently, scattering of PKP and PKKP precursors can be modeled with ~300 m RMS height topography (Earle & Shearer 1997, Shearer et al 1998). Also, antipode PKP data suggest limited, small-amplitude topography, at least in some regions (Poupinet et al 1993). Large uncertainties related to CMB topography/roughness are present (Pulliam & Stark 1993, Garcia & Souriau 2000). One study based on PcP observations and synthetics argues that topography, if present, should not exceed 2–3 km in amplitude (Neuberg & Wahr 1991). CMB roughness as well as long wavelength topography is likely to be intimately linked to ULVZ boundary layer structure, if present. Again, a multiphase approach is desired, whereby phases sensitive to CMB roughness and CMB boundary layer structure can be analyzed for the same CMB region.

In most cases, topography trades off with heterogeneity just above the boundary. Nonetheless, detailed studies of the structure right at the base of the mantle—in particular, P-wave structure—indicate strong heterogeneity just at or above the CMB (e.g. Doornbos & Hilton 1989, Sylvander & Souriau 1996b, Obayashi & Fukao 1997, Sylvander et al 1997). Better resolution regarding characterization of heterogeneity right at the CMB is important because it relates not only to ULVZ work but also to the issue of core-mantle coupling—for example, topographic (e.g. Hide et al 1993) or electromagnetic (Aurnou et al 1996, Buffett 1998, Holme 1998). This is a truly far-reaching consequence of possible chemical heterogeneity in the lowermost mantle (and/or the boundary between the mantle and core), with potential effects on the magnetic field at the surface (e.g. Jeanloz 1990, Poirier & le Mouël 1992, Gubbins 1994) as well as length of day. Recently, however, it has been suggested that a conducting layer is unlikely to be greater than a few tens of meters (Poirier et al 1998), and that heterogeneity in lowermost mantle electrical conductivity should not strongly affect polarity reversals (Brito et al 1999).

Relationship to Overlying Mantle

Preliminary evidence exists for a relationship between the presence of UVLZs and overlying depressed D″ velocities (Garnero & Helmberger 1995b). Because of coverage (or resolution) limitations, however, the potential pervasiveness of this relationship has not been established. Combining information from different seismic phases will ultimately help—e.g. scattering implied from PKP precursors combined with basal layering inferred from SPdKS or PcP and ScP precursors. Sampling one CMB region with different phases requires fortuitous source-receiver geometries, because different phases have different distance ranges of utility for ULVZ study. Nonetheless, low velocities in D″ (implied from either raw travel times, Figure 2, or solution maps from tomography, Figure 5) are pervasive beneath the central Pacific and western Africa. ULVZ structure has been proposed for these areas, particularly beneath the Pacific where path coverage is more extensive.

The depth to which low-velocity structures extend up into the lower mantle has received attention recently, because this may relate to upwellings, or ''superplumes.'' Using forward modeling of differential travel times sensitive to deep mantle structure, and with the aid of a starting model from tomographic studies, Ritsema et al (1998) and Bréger & Romanowicz (1998) both have presented evidence for low shear velocities (3%–4%) extending far up into the lower mantle. In a tomographic inversion of ISC P phases, Bijwaard & Spakman (1999) present a model with connectivity of low velocities from crust to CMB, beneath Iceland. The shape of these proposed structures is illustrated in schematic cross-sections in Figure 11 (color insert). Only the strongest heterogeneity is shown. The degree of thermal versus chemical component to these structures is not yet established. It is remarkable that each of these overlie ULVZ, which suggests a causal relationship, as is argued for in Williams et al (1998).

DISCUSSION

We have seen evidence for strong heterogeneity in the deepest mantle at many wavelengths. Raw differential travel times (Figures 2, 3, and 4) exhibit varying scale lengths of heterogeneity, from long to short wavelength, depending on the length of path in the D″ region. The longest D″ paths are in the diffracted phases, so the smoothed Sdiff-SKS and Pdiff-PKP times display the most coherent large-scale variations (Figure 2), which resemble long-wavelength tomographic inversion results. ScS paths are shorter in D″, and smoothed times display shorter scale variations. As mentioned, however, the accompanying direct S-waves in ScS-S times bottom far above the CMB at shorter epicentral distances (Figure 1*a*), which may result in mid-mantle contamination to that time (if not properly accounted for). The importance of understanding some of the uncertainties in lowermost mantle seismic studies cannot be overemphasized; we briefly discuss this next.

Seismic Resolution and Uncertainty

Many difficulties arise in forward and inverse studies of seismic structure because of resolution and uncertainty issues. In many cases, there is a large solution space of viable models that explain waveform and/or travel time behavior equally well. For many studies, particularly those using radially symmetric Earth models to predict ray paths (i.e. 1-D, which includes much of this author's past work), uncertainties can arise due to lack of knowledge of the actual raypath in the presence of strong heterogeneity and lateral gradients. Although these effects are starting to be addressed (e.g. Weber 1993; Igel & Weber 1996; Schimmel & Paulssen 1996; Helmberger et al 1996a,b; Thomas & Weber 1997; Wen & Helmberger 1998), a majority of studies still use 1-D methods in describing deep mantle heterogeneity. This is clearly an area slated for improvement in future work.

Probably the single most important factor contributing to lack of resolution in seismic structure studies is poor (or less than ideal) raypath coverage of the study area. Important path coverage issues include (*a*) lateral and radial density of raypaths in the region of interest; (*b*) degree of crossing raypaths; and (*c*) length of path in the structure of interest, which relates to potential smearing in the absence of adequate crossing-path coverage. In the presence of strong heterogeneity, which clearly exists at the base of the mantle (Figures 2 through 5), accurate estimation of ray path location using 1-D methods is at best limited to longer wavelengths, making confident seismic structure retrieval at short scales difficult. For example, models of D″ structure can be strongly biased by non-1-D mantle structure (e.g. Figure 9). Thomas & Weber (1997) show strong effects on the P-wave field for topographical heterogeneity, suggesting D″ topography of 10–100 km with lateral wavelengths of 400–1200 km. Such topography could contribute to the sometimes intermittent observation of the reflection off the high velocity D″ structure, as documented by Lay and coworkers. Other 3-D effects include upper mantle contamination of arrivals by phenomena such as slab diffraction (e.g. Cormier 1988, Vidale 1987).

Examples of possible smearing of deep mantle structure include regions beneath the Caribbean (South American earthquakes recorded in North America: a north/south corridor), Alaska (northwest Pacific subduction zone events recorded in North America: an east-west corridor), and central Pacific (southwest Pacific events recorded in North America: a SW-NE corridor). Potential streaking of strong heterogeneity can be minimized only by crossing path coverage or by paths that travel vertically through the region of interest. Such is the case for the Caribbean corridor in the upper part of the lower mantle—for example, in the study by Grand (1994) where multiple S bounce data and SKS add constraints to lateral placement of anomalies along the corridor. Underestimation of heterogeneity strength is possible in the presence of poor, along-azimuth crossing path coverage. These problems can be confounded with global spherical harmonic expansion of heterogeneity, where regions containing no coverage whatsoever are assigned aspherical structure. Problems may also arise from errors in the reference model (particularly the crust) and unaccounted-for topography on significant internal boundaries (see discussion by Ritzwoller & Lavely 1995).

Thermal and Chemical Considerations for Origin of Heterogeneity

The origin of deep mantle heterogeneity has long been speculated. Because we have little means of acquiring mineral samples directly from the region, the remote sensing tool of seismology has been the predominant method for mapping and interpreting the heterogeneity. Recently, achieving global coverage in the deep mantle for P and S structure has been greatly improved, at least at long wavelength (e.g. Figure 5). Many of these studies (e.g. Kumagai et al 1992; Robertson & Woodhouse 1995, 1996; Bolton 1996; Vasco & Johnson 1998; Kennett et al 1998), as well as forward modeling methods (e.g. Wysession et al 1992, 1993, 1999), have shown the breakdown in correlation between P and S velocity heterogeneity in the deep mantle. This suggests that thermal anomalies alone cannot explain the heterogeneity, which points to the possibility of some chemical signature that may be due to Fe enrichment (e.g. Wysession et al 1999). Other studies have compared P and S structural details, e.g. the D″ discontinuity (Weber & Davis 1990, Weber 1993), velocity gradients [e.g. beneath the central Pacific, $\partial V_P/\partial z$ of Young & Lay (1989) is positive, whereas $\partial V_P/\partial z$ of Ritsema et al (1997) is steeply negative]. Devising experiments that use redundant P and S waves with similar paths (as in Bina & Silver 1997) can potentially help in sorting out chemical versus thermal origin for heterogeneity.

As mentioned earlier, small-scale heterogeneity at or near the CMB (e.g. ULVZ) may be due to partial melt. Although considerations of the geotherm have argued that perovskite, the supposed dominant lower mantle mineral, should not melt because of high melting temperature estimations (Zerr & Boehler 1993, Boehler 1996, Serghiou et al 1998), some experimental high pressure studies have affirmed the feasibility of lowermost mantle melt (e.g. Holland & Ahrens 1997, Zerr et al 1998). The possibility of mantle olivine becoming denser upon melt, and thus sinking to the CMB, has also been proposed (Knittle 1998). Discussion of melting at the base of the mantle depends on the temperature drop across D″, which strongly depends on the inferred temperature of the inner core–outer core boundary. Uncertainties in this number permits a significant range in possible temperature drops across D″ (Williams 1998). Establishing a 3-to-1 δV_S-to-δV_P ratio for mantle-side CMB heterogeneity (or a ULVZ) with other than indirect means is difficult, though indirect methods have shown that the 3-to-1 ratio is compatible with various data types (Revenaugh & Meyer 1997, Helmberger et al 1998, Vidale & Hedlin 1998, Wen & Helmberger 1998).

The geodynamical modeling community has been aware of the importance of the lithosphere and plates for the behavior of mantle convection (e.g. Davies 1988, Gurnis 1988). Lowermost mantle structure and processes similarly have relationships to important mantle processes, such as plume formation. For example, large, low seismic velocity anomalies that extend into the lower mantle (''super-plumes'') have been modeled as thermal anomalies (e.g. Thompson & Tackley 1998). Other interesting phenomena, such as plume-plume collisions that produce super-plumes (Brunet & Yuen 2000), have been demonstrated as a CMB possibility. In a combination of seismological and geodynamical analyses, Kellogg et al (1999) and van der Hilst & Kárason (1999) argue for a layer of chemical heterogeneity in the lower 1000 km or so of the mantle. They hypothesize that this layer may be a reservoir of elements that are depleted from the upper mantle. Kaneshima & Helffrich (1998) support this idea with detection of mid-lower mantle reflections. Super-fast mantle plumes (Larsen et al 2000) are yet another potential connection between the deep Earth and the rest of the mantle. It's very likely that the deep mantle is intimately related to the mode of mantle mixing—for example, episodic flushing of upper mantle slab material into the lower mantle (e.g. Tackley et al 1993).

A strong correlation has been identified between proposed ultra-low velocity zone locations and hotspot surficial locations (Williams et al 1998), implying a causal relationship between ULVZ and mantle plumes. The hypothesis that some plume sources may come from the deep mantle is consistent with implications from the study of osmium ratios, which imply that a small fraction of outer core has been entrained in mantle plumes (Brandon et al 1998). Other evidence exists for a lower mantle source for at least some plumes seen at the surface (Ribe & de Valpine 1994). For example, the Iceland plume appears to be well modeled with a CMB source (e.g. Wolfe et al 1997, Shen et al 1998, Helmberger et al 1998, Bijwaard & Spakman 1999). An important parameter is the excess temperature of plumes compared to the surrounding mantle, which is far less than that noted for the thermal boundary layer at the CMB (e.g. 200–300°C compared to 1000–1300°C, respectively). This parameter has been used to imply that a thin mantle basal chemical layer may exist if plumes originate at the CMB (Farnetani 1997). With plumes possibly linked to a wide variety of phenomena, such as magnetic reversal frequency (e.g. Larson & Olson 1991), it is clear that a better understanding of lower mantle structure and dynamics will help to elucidate whole Earth dynamics and evolution.

The CMB represents the largest absolute increase in density anywhere in the planet. This boundary provides for a repository of material having a density between those of the mantle and core. Depending on the vigor of convection and density of reaction products, D″ may contain significant chemical heterogeneity in some regions (e.g. Knittle & Jeanloz 1991, Kellogg & King 1993, Kellogg 1997). Whether or not this heterogeneity can form into a stable, chemically distinct layer over geologic time periods depends on many factors, and is still an area of active research. For example, a chemically distinct layer can stabilize the location of roots of upwellings, as well as affect core heat flux across the CMB (Montague et al 1998). Additionally, possible chemical reactions between the mantle and core (Knittle & Jeanloz 1989, 1991) allow for scenarios of chemical heterogeneity in the lowermost mantle, and serve to make the CMB a gradational boundary over some finite depth interval (e.g. 1.5 km, Garnero & Jeanloz 2000). Such chemical anomalies, if strongly iron-bearing, may affect Earth's magnetic field through coupling between the field and conducting lowermost mantle heterogeneity (Jeanloz 1990, Buffett 1998, Lister & Buffett 1998).

Does subducted material retain its character in some form to cause D″ phenomena observed below the locations of past and present subduction zones? Many hypotheses have been put forth that contain slab scenarios of involvement in D″ (e.g. for summaries, see Loper & Lay 1995, Wysession 1996b, Lay et al 1998a). A common example is the possibility of former oceanic crust subducting into the lower mantle and partially melting at the base of the mantle (Hirose et al 1999), which may relate to either ULVZ origin (e.g. Garnero et al 1998) or D″ anisotropy (e.g. Kendall & Silver 1996, 1998).

Large uncertainties are present in lowermost mantle structure and dynamics (D″ discontinuity and anisotropy, scatterers, ULVZ, CMB topography and transitional structure, dynamical motions). This makes accurate description of the source of lower mantle heterogeneity, as well as its time evolution, rather difficult at best. For this reason, these uncertainties are present in scenarios containing even basic chemical, thermal, and dynamical lowermost mantle components. Nonetheless, we present a hypothetical scenario containing some of the proposed features that may be present in the lowermost mantle beneath low-velocity (warm?) regions, such as the central Pacific (Figure 12, color insert). ULVZ structure may contain various types of stratification: a mantle-side component of partial melt right at the CMB, chemical heterogeneity in the ULVZ and possibly above, a thin mantle-to-core transition between the mantle and core, and outermost core thin zones of rigidity beneath upwarpings of the CMB. Local topographical highs may concentrate under dynamic upwellings that are roots of mantle plumes. Small scatterers of melt and/or chemical heterogeneity may be concentrated near the CMB in these most anomalous zones, which may extend up into D″. Strong lateral flow that feeds the plumes can align either crystals, pockets or films of melt, or some other type of heterogeneity, to give rise to D″ anisotropy. A coherent lateral surface of such alignments, or possibly a phase change, can give rise to a D″ discontinuity.

A contrasting picture to that described above would accompany regions of high velocities in D″, such as that beneath many present or past subduction zones (e.g. the circum-Pacific). In such regions, ULVZ layering as depicted in Figure 12 should be absent or greatly reduced in thickness (i.e. unobservable). The CMB should be isothermal, so any partial melt of an iso-chemical mantle in contact with the core should be global. The thickness of a global melt layer might be reduced to a 10–100 meter scale—which would be virtually invisible to present seismic methods. Alternatively, lateral differences in lower mantle chemistry, as previously discussed, could result in no ULVZ structure at all in these high-velocity regions. In these regions, strong support for anisotropy and D″ discontinuities is present, and evidence is lacking for any enhancement of scatterers (from PKP precursors) or plume roots (from isolated low velocities).

Future Work

In order to make advancements in imaging or characterizing the lower mantle, progress must be made in all pertinent disciplines, such as seismology, geodynamics, mineral physics, geodetics, and geomagnetics. In seismology, improvements are necessary in data set collection, wave propagation methods, and theoretical methods (e.g. inversion). Advancements in all these areas are rapidly taking place, and are in fact redefining our ideas of deep Earth structure and dynamics every few years or so. Another drawback is that we unfortunately have no direct means of sampling the mineralogy of Earth's lowermost mantle. Therefore, laboratory experiments on proposed lower mantle constituent material or analogs, as well as theoretical efforts, must be carried out (e.g. see review by Bina 1998).

With the advent of portable dense high-quality arrays (e.g. Wysession et al 1996), higher order information (spatial patterns at much smaller scale) are pursuable, which presents us with the opportunity to relate detailed findings to previously mapped larger scale structures. The benefits of dense data arrays have been demonstrated by many (e.g. Weber 1993, Weber et al 1996, Revenaugh & Meyer 1997), along with stacking large data sets of high-quality digital data (e.g. see Astiz et al 1996). Future forward modeling studies of deep mantle heterogeneity will surely incorporate such data. Bridging the gap between small- and large-scale, seismically imaged features should significantly help Earth scientists make the link between the ''reds and blues'' of long wavelength seismology, small-scale phenomena from regional studies, and the dynamics of Earth's deep interior inferred from numerical work. We wish to move beyond our present ''snapshot'' image of the structure of Earth's interior, toward better understanding of Earth evolution and dynamics.

Unlocking the mystery of the cause/origin of seismic anisotropy should improve our understanding of the source of heterogeneity, at least for small to intermediate scales. Better documenting trends in V_{SH} compared to V_{SV} will help in this regard (e.g. see Karato 1998, Kendall & Silver 1998, Lay et al 1998b). Similarly, we wish to better understand the distribution and cause of CMB boundary layer heterogeneity (i.e ULVZ). Does the lower mantle that overlies these zones contain the same small-scale lateral variations in heterogeneity? Answering this question will require more than one type of seismic phase sampling of the region of interest—and preferably dense sampling. Better understanding the origin of these ultra-lowered wavespeeds will be key in understanding lowermost mantle dynamics and other important topics such as plume initiation (e.g. see Kellogg & King 1997).

CONCLUSION

Seismology is one of the best tools for probing the inaccessible regions of the deep Earth. Many useful analyses and data are available, and can be grouped according to forward and inverse approaches. Inverse methods, such as tomography, yield long-wavelength (e.g. $>$1000–3000 km) variations of deep mantle lateral heterogeneity, with vertical variations smoothly varying over hundreds of km. Forward methods, such as analyses of differential travel times, provide detailed structural information on topics such as D″ heterogeneity, discontinuity, anisotropy, and scattering, as well as ultra-low velocities associated with the CMB. Reconciling these various structures into a coherent scenario is difficult, owing to uncertainties and lack of detailed resolution. Possibilities include combinations of thermal, chemical, and phase change explanations for D″ heterogeneity and discontinuity, aligned crystals, heterogeneity, or melt for D″ anisotropy, and partial melt and chemical heterogeneity for the ultra-low velocity zone. Better seismic wavepath coverage, coupled with multiphase analyses, will provide added constraints in the seismic studies. This, combined with continued advances in the related fields of geodynamics, mineral physics, geodetics, and geomagnetics, will help to add the necessary constraints for reducing uncertainties in solution models; this should pave the way for more confident statements regarding the origin of lowermost mantle heterogeneity.

ACKNOWLEDGMENTS

Special thanks to H Bijwaard, L Bréger, J Castle, S Grand, H Karason, B Kuo, G Laske, T Lay, X-F Liu, G Masters, C Megnin, J Ritsema, B Romanowicz, S Russell, A Souriau, W-J Su, M Sylvander, H Tckalcic, R van der Hilst, D Vasco, M Weber, and M Wysession, who sent me raw data sets, models, images, and processing codes. This work benefited from the many conversations with the above and also D Helmberger, R Jeanloz, and Q Williams. EJG was partially supported by NSF grant EAR-9996302.

Visit the Annual Reviews home page at www.AnnualReviews.org.

LITERATURE CITED

Astiz L, Earle P, Shearer PM. 1996. Global stacking of broadband seismograms. *Seismol. Res. Lett.* 67:8–18

Aurnou J, Buttles JL, Numann GA, Olson PL. 1996. Electromagnetic core-mantle coupling and paleomagnetic reversal paths. *Geophys. Res. Lett.* 19:2705–8

Bataille K, Lund F. 1996. Strong scattering of short-period seismic waves by the core-mantle boundary and the P-diffracted wave. *Geophys. Res. Lett.* 18:2413–16

Bataille K, Wu RS, Flatte S. 1990. Inhomogeneities near the core-mantle boundary evidenced from scattered waves: a review. *Pageoph.* 132:151–73

Bijwaard H, Spakman W. 1999. Tomographic evidence for a narrow whole mantle plume below Iceland. *Earth Planet. Sci. Lett.* 166:121–66

Bijwaard H, Spakman W, Engdahl ER. 1998. Closing the gap between regional and global travel time tomography. *J. Geophys. Res.* 103:30055–78

Bina CR. 1998. Lower mantle mineralogy and the geophysical perspective. In *Ultrahigh-pressure Mineralogy, Physics and Chemistry of the Earth's Deep Interior,* ed. R Hemley, pp. 205–39. Washington, DC: Mineral. Soc. Am.

Bina CR, Silver PG. 1997. Bulk sound travel times and implications for mantle composition and outer core heterogeneity. *Geophys. Res. Lett.* 24:499–503

Boehler R. 1996. Melting temperature of the Earth's mantle and core: Earth's thermal structure. *Annu. Rev. Earth Planet. Sci.* 24:15–40

Bolton HF. 1996. *Long period travel times and the structure of the mantle.* PhD thesis. University of California, San Diego. 235 pp.

Bowers D, McCormack DA, Sharrock DS. 2000. Observations of PKP(DF) and PKP(BC) across the United Kingdom—implications for studies of attenuation in the Earth's core. *Geophys. J. Int.* In review

Brandon AD, Walker RJ, Morgan JW, Norman MD, Prichard HM. 1998. Coupled ^{186}Os and ^{187}Os evidence for core-mantle interaction. *Science* 280:1570–73

Bréger L, Romanowicz B. 1998. Three-dimensional structure at the base of the mantle beneath the central Pacific. *Science* 282:718–20

Bréger L, Tkalcic H, Romanowicz B. 2000. The effect of D″ on PKP(AB-DF) travel time residuals and possible implications for inner core structure. *Earth Planet. Sci. Lett.* Submitted

Brito D, Aurnou J, Olson P. 1999. Can heterogeneous core-mantle electromagnetic coupling control geomagnetic reversals? *Phys. Earth Planet. Int.* 112:159–70

Brunet D, Yuen DA. 2000. Dynamics of plumes and superplumes governed by mantle phase transitions and variable viscosity. *Earth Planet. Sci. Lett.* In review

Buffett BA. 1998. Free oscillations in the length of day: inferences on physical properties near the core-mantle boundary. In *The Core-Mantle Boundary,* ed. M Gurnis, ME Wysession, E Knittle, BA Buffett, pp. 153–65. Washington, DC: AGU

Bullen KE. 1949. Compressibility-pressure hypothesis and the Earth's interior. *MNRAS, Geophys. Suppl.* 5:355–68

Castle JC, Creager KC, Winchester JP, van der Hilst RD. 2000. Shear wave velocity structure at the base of the mantle. *J. Geophys. Res.* In press

Cormier VF. 1988. Slab diffraction of seismic waves. *J. Geophys. Res.* 94:3006–24

Cormier VF. 1999. Anisotropy of heterogeneity scale lengths in the lower mantle from PKIKP precursors. *Geophys. J. Int.* 136:373–84

Davies GF. 1988. Role of the lithosphere in mantle convection. *J. Geophys. Res.* 93:10451–66

Doornbos DJ, Hilton T. 1989. Models of the core-mantle boundary and the travel times of internally reflected core phases. *J. Geophys. Res.* 94:15741–51

Dziewonski AM. 1984. Mapping the lower mantle: determination of lateral heterogeneity in P velocity up to degree and order 6. *J. Geophys. Res.* 89:5929–52

Dziewonski AM. 1996. Earth's mantle in three dimensions. In *Seismic Modeling of Earth Structure,* ed. E Boschi, G Ekstrom, A Morelli, pp. 507–72. New York: North-Holland

Dziewonski AM, Anderson DL. 1981. Preliminary Reference Earth Model. *Phys. Earth Planet Int.* 25:297–356

Earle PS, Shearer PM. 1997. Observations of PKKP precursors used to estimate small-scale topography on the core-mantle boundary. *Science* 277:667–70

Earle PS, Shearer PM. 1998. Observations of high-frequency scattered energy associated with the core phase PKKP. *Geophys. Res. Lett.* 25:405–8

Engdahl ER, van der Hilst R, Buland R. 1998. Global teleseismic earthquake relocation with improved travel times and procedures for depth determination. *Bull. Seismol. Soc. Am.* 88:722–43

Farnetani CG. 1997. Excess temperature of mantle plumes: the role of chemical stratification across D″. *Geophys. Res. Lett.* 24:1583–86

Fukao Y. 1992. Seismic tomogram of the Earth's mantle: geodynamic implications. *Science* 258:625–30

Garcia R, Souriau A. 2000. Amplitude of the core mantle boundary topography estimated by stochastic analysis of core phases. *Phys. Earth Planet. Int.* In press

Garnero EJ, Helmberger DV. 1993. Travel times of S and SKS: implications for three-dimensional lower mantle structure beneath the central Pacific. *J. Geophys. Res.* 98:8225–41

Garnero EJ, Helmberger DV. 1995a. On seismic resolution of lateral heterogeneity in the Earth's outermost core. *Phys. Earth Planet. Int.* 88:117–30

Garnero EJ, Helmberger DV. 1995b. A very slow basal layer underlying large-scale low-velocity anomalies in the lower mantle beneath the Pacific: evidence from core phases. *Phys. Earth Planet. Int.* 91:161–76

Garnero EJ, Helmberger DV. 1998. Further constraints and uncertainties in modeling a mantle basal layer of ultra-low velocities. *J. Geophys. Res.* 103:12495–509

Garnero EJ, Helmberger DV, Grand SP. 1993. Constraining outermost core velocity with SmKS waves. *Geophys. Res. Lett.* 22:2463–66

Garnero EJ, Jeanloz R. 2000. Fuzzy patches on the Earth's core-mantle boundary? *Geophys. Res. Lett.* In review

Garnero EJ, Lay T. 1999. Anisotropy in D″: assessing the lamellae hypothesis. *Eos Trans. Am. Geophys. Union* 80:512

Garnero EJ, Revenaugh JS, Williams Q, Lay T, Kellogg LH. 1998. Ultralow velocity zone at the core-mantle boundary. In *The Core-Mantle Boundary,* ed. M Gurnis, ME Wysession, E Knittle, BA Buffett, pp. 319–34. Washington, DC: AGU

Grand SP. 1994. Mantle shear structure beneath the Americas and surrounding oceans. *J. Geophys. Res.* 99:11591–621

Grand SP, van der Hilst RD, Widiyantoro S. 1997. Global seismic tomography: a snapshot of convection in the Earth. *GSA Today* 7:1–7

Gubbins D. 1994. Geomagnetic polarity reversals: a connection with secular variation and core-mantle interaction. *Rev. Geophys.* 32:61–83

Gurnis M. 1988. Large-scale mantle convection and the aggregation and dispersal of supercontinents. *Nature* 332:1–5

Hager BH, Clayton RW, Richards MA, Comer RP, Dziewonski AM. 1985. Lower mantle heterogeneity, dynamic topography and the geoid. *Nature* 313:541–45

Hansen U, Yuen DA. 1988. Numerical simulations of thermal-chemical instabilities at the core-mantle boundary. *Nature* 334:237–40

Hedlin MAH, Shearer PM. 2000. An analysis of large-scale variations in small-scale mantle heterogeneity using GSN recordings of precursors to PKP. *J. Geophys. Res.* In press

Hedlin MAH, Shearer PM, Earle PS. 1997. Seismic evidence for small-scale heterogeneity throughout the Earth's mantle. *Nature* 387:145–50

Helmberger DV. 1983. Theory and application of synthetic seismograms. In *Earthquakes: Observation, Theory, and Interpretation,* ed. H Kanamori, E Boschi. 37:174–217 Rome, Italy: Istituto Nazionale di Geofisica

Helmberger DV, Garnero EJ, Ding X-D. 1996a. Modeling two-dimensional structure at the core-mantle boundary. *J. Geophys. Res.* 101:13963–72

Helmberger DV, Wen L, Ding X. 1998. Seismic evidence that the source of the Iceland hotspot lies at the core-mantle boundary. *Nature* 396:251–55

Helmberger DV, Zhao L-S, Garnero EJ. 1996b. Construction of synthetics for 2-D structures; core phases. In *Seismic Modeling of Earth Structure,* ed. E Boschi, G Ekstrom, A Morelli, pp. 183–222. New York: North-Holland

Hide R, Clayton RW, Hager BH, Spieth MA, Voorhies CV. 1993. Topographic core-mantle coupling and fluctuations in the Earth's rotation. In *Relating Geophysical Structures and Processes: The Jeffreys Volume,* ed. K Aki, R Dmowska. p. 107. Washington, DC: AGU

Hirose K, Fei Y, Ma Y, Mao H-K. 1999. The fate of subducted basaltic crust in the Earth's lower mantle. *Nature* 397:53–56

Holland KG, Ahrens TJ. 1997. Melting of (Mg,Fe)2SiO4 at the core-mantle boundary of the Earth. *Science* 275:1623–25

Holme R. 1998. Electromagnetic core-mantle coupling II: probing deep mantle conductance. In *The Core-Mantle Boundary,* ed. M Gurnis, ME Wysession, E Knittle, BA Buffett, pp. 139–54. Washington, DC: AGU

Houard S, Nataf H-C. 1993. Laterally varying reflector at the top of D″ beneath northern Siberia. *Geophys. J. Int.* 115:168–82

Igel H, Weber M. 1996. P-SV wave propagation in the Earth's mantle using finite differences: application to heterogeneous lowermost mantle structure. *Geophys. Res. Lett.* 23:415–18

Jeanloz R. 1990. The nature of the Earth's core. *Annu. Rev. Earth Planet. Sci.* 18:357–86

Kanamori H. 1967. Spectrum of P and PcP in relation to the mantle-core boundary and attenuation in the mantle. *J. Geophys. Res.* 72:559

Kaneshima S, Helffrich G. 1998. Detection of lower mantle scatterers northeast of the Marianna subduction zone using short-period array data. *J. Geophys. Res.* 103:4825–38

Karato S-I. 1989. Plasticity-crystal structure systematics in dense oxides and its implications for the creep strength of the Earth's deep interior: a preliminary result. *Phys. Earth Planet. Int.* 55:234–40

Karato S-I. 1998. Some remarks on the origin of seismic anisotropy in the D″ layer. *Earth Planets Space* 50:1019–28

Kellogg LH. 1997. Growing the Earth's D″ layer: effect of density variations at the core-mantle boundary. *Geophys. Res. Lett.* 24:2749–52

Kellogg LH, Hager BH, van der Hilst RD. 1999. Compositional stratification in the deep mantle. *Science* 283:1881–84

Kellogg LH, King SD. 1993. Effect of mantle plumes on the growth of D″ by reaction between the core and mantle. *Geophys. Res. Lett.* 20:379–82

Kellogg LH, King SD. 1997. The effect of temperature dependent viscosity on the structure of new plumes in the mantle: results of a finite element model in a spherical, axisymmetric shell. *Earth Planet. Sci. Lett.* 148:13–26

Kendall JM, Shearer PM. 1994. Lateral variations in D″ thickness from long-period shear wave data. *J. Geophys. Res.* 99:11575–90

Kendall JM, Shearer PM. 1995. On the structure of the lowermost mantle beneath the southwest Pacific, southeast Asia and Australasia. *Phys. Earth Planet. Int.* 92:85–98

Kendall JM, Silver PG. 1996. Constraints from seismic anisotropy on the nature of the lowermost mantle. *Nature* 381:409–12

Kendall JM, Silver PG. 1998. Investigating causes of D″ anisotropy. In *The Core-Mantle Boundary,* ed. M Gurnis, ME Wysession, E Knittle, BA Buffett, pp. 97–118. Washington, DC: AGU

Kennett BLN, Engdahl ER. 1991. Traveltimes for global earthquake location and phase identification. *Geophys. J. Int.* 105:429–65

Kennett BLN, Widiyantoro S, van der Hilst RD. 1998. Joint seismic tomography for bulk sound and shear wave speed in the Earth's mantle. *J. Geophys. Res.* 103:12469–93

Knittle E. 1998. The solid/liquid partitioning of major and radiogenic elements at lower mane pressures: implications for the core-mantle boundary region. In *The Core-Mantle Boundary,* ed. M Gurnis, ME Wysession, E Knittle, BA Buffett, pp. 119–30. Washington, DC: AGU

Knittle E, Jeanloz R. 1989. Simulating the core-mantle boundary: an experimental study of high-pressure reactions between silicates and liquid iron. *Geophys. Res. Lett.* 16:609–12

Knittle E, Jeanloz R. 1991. Earth's core-mantle boundary: results of experiments at high pressures and temperatures. *Science* 251:1438–43

Krüger F, Weber M, Scherbaum F, Schlittenhardt J. 1995. Evidence for normal and inhomogeneous lowermost mantle and core-mantle boundary structure under the Arctic and northern Canada. *Geophys. J. Int.* 122:637–57

Kumagai H, Fukao Y, Suda N, Kobayashi N. 1992. Structure of the D″ layer inferred from the Earth's free oscillations. *Phys. Earth Planet. Sci.* 73:38–52

Kuo B-Y. 2000. Amplitude of Sd across Asia: effects of velocity gradient and Qs in the D″ region and the asphericity of the mantle. *J. Geophys. Res.* In review

Kuo B-Y, Wu K-Y. 1997. Global shear velocity heterogeneities in the D″ layer: inversion from Sd-SKS differential travel times. *J. Geophys. Res.* 102:11775–88

Kuo B-Y, Garnero EJ, Lay T. 2000. Global shear velocity heterogeneity in D″ from tomographic inversion of S-SKS times. *J. Geophys. Res.* Submitted

Larsen TB, Yuen DA, Storey M. 2000. Ultrafast mantle plumes and implications for flood basalt volcanism in the northern Atlantic region. *Tectonophys.* In press

Larson RL, Olson P. 1991. Mantle plumes control magnetic reversal frequency. *Earth Planet. Sci. Lett.* 107:437–47

Lay T, Helmberger DV. 1983. A lower mantle S-wave triplication and the shear velocity structure of D″. *Geophys. J. R. Astron. Soc.* 75:799–838

Lay T, Garnero EJ, Williams Q, Kellogg L, Wysession ME. 1998b. Seismic wave anisotropy in D″ and its implications. In *The Core-Mantle Boundary,* ed. M Gurnis, ME Wysession, E Knittle, BA Buffett, pp. 299–318. Washington, DC: AGU

Lay T, Garnero EJ, Young CJ, Gaherty JB. 1997. Scale lengths of shear velocity heterogeneity at the base of the mantle from S wave differential travel times. *J. Geophys. Res.* 102:9887–909

Lay T, Young CJ. 1990. The stably-stratified outermost core revisited. *Geophys. Res. Lett.* 17:2001–4

Lay T, Young CJ. 1996. Imaging scattering structures in the lower mantle by migration of long-period S waves. *J. Geophys. Res.* 101:20023–40

Lay T, Williams Q, Garnero EJ. 1998a. The core-mantle boundary layer and deep earth dynamics. *Nature* 392:461–68

Li X-D, Romanowicz B. 1996. Global mantle shear-velocity model developed using nonlinear asymptotic coupling theory. *J. Geophys. Res.* 101:22245–72

Lister JR, Buffett BA. 1998. Stratification of the outer core at the core-mantle boundary. *Phys. Earth Planet. Int.* 105:5–19

Lithgow-Bertelloni C, Richards MA. 1998. The dynamics of Cenozoic and Mesozoic plate motions. *Rev. Geophys.* 36:27–78

Liu X-F, Dziewonski AM. 1994. Lowermost mantle shear wave velocity structure. *EOS Trans. AGU Fall Supplement.* 75:663

Liu X-F, Dziewonski AM. 1998. Global analysis of shear wave velocity anomalies in the lower-most mantle. In *The Core-Mantle Boundary*, ed. M Gurnis, ME Wysession, E Knittle, BA Buffett, pp. 21–36. Washington, DC: AGU

Loper DE, Lay T. 1995. The core-mantle boundary region. *J. Geophys. Res.* 100:6397–420

Manga M, Jeanloz R. 1996. Implications of a metal-bearing chemical boundary layer in

D″ for mantle dynamics. *Geophys. Res. Lett.* 23:3091–94

Masters G, Johnson S, Laske G, Bolton H. 1996. A shear-velocity model of the mantle. *Philos. Trans. R. Soc. Lond. A* 354:1385–411

Matzel EM, Sen K, Grand SP. 1996. Evidence for anisotropy in the deep mantle beneath Alaska. *Geophys. Res. Lett.* 23:2417–20

Mitchell BJ, Helmberger DV. 1973. Shear velocities at the base of the mantle from observations of S and ScS. *J. Geophys. Res.* 78:6009–20

Montagner J-P. 1998. Where can seismic anisotropy be detected in the Earth's mantle? In boundary layers . . . *Pure Appl. Geophys.* 151:223–56

Montague NL, Kellogg LH, Manga M. 1998. High Rayleigh number thermo-chemical models of a dense boundary layer in D″. *Geophys. Res. Lett.* 25:2345–48

Nagumo S, McCreery CS. 1992. PcP and ScP beneath the western Pacific detected by a deep ocean bottom hydrophone array. *Geophys. Res. Lett.* 15:1559–62

Nataf H-C, Houard S. 1993. Seismic discontinuity at the top of D″: a world-wide feature? *Geophys. Res. Lett.* 20:2371–74

Neuberg J, Pointer T. 1995. Modelling seismic reflections from D″ using the Kirchhoff method. *Phys. Earth Planet. Int.* 90:273–81

Neuberg J, Wahr J. 1991. Detailed investigation of a spot on the core-mantle boundary using digital PcP data. *Phys. Earth Planet. Int.* 68:132–43

Obayashi M, Fukao Y. 1997. P and PcP travel time tomography for the core-mantle boundary. *J. Geophys. Res.* 102:17825–41

Pointer T, Neuberg J. 1995. Deconvolution of overcritical P-wave reflections from the top of D″. *Phys. Earth Planet. Int.* 90:283–301

Poirier P, le Mouël JL. 1992. Does infiltration of core material into the lower mantle affect the observed geomagnetic field? *Phys. Earth Planet. Int.* 73:29–37

Poirier JP, Malavergne V, le Mouël JL. 1998. Is there a thin electrically conducting layer at the base of the mantle? In *The Core-Mantle Boundary*, ed. M Gurnis, ME Wysession, E Knittle, BA Buffett, pp. 131–41. Washington, DC: AGU

Poupinet G, Souriau A, Jenatton A. 1993. A test on the Earth's core-mantle boundary structure with antipodal data: example of Fiji-Tonga earthquakes recorded in Tamanrasset, Algeria. *Geophys. J. Int.* 113:684–92

Pulliam RJ, Stark PB. 1993. Bumps on the core-mantle boundary: Are they facts or artifacts? *J. Geophys. Res.* 98:1943–55

Reasoner C, Revenaugh J. 1999. Short-period P wave constraints on D″ reflectivity. *J. Geophys. Res.* 104:955–62

Revenaugh JS, Meyer R. 1997. Seismic evidence of partial melt within a possibly ubiquitous low-velocity layer at the base of the mantle. *Science* 277:670–73

Ribe NM, de Valpine DP. 1994. The global hotspot distribution and instability of D″. *Geophys. Res. Lett.* 21:1507–10

Ritsema J, Garnero EJ, Lay T. 1997. A strongly negative shear velocity gradient and lateral variability in the lowermost mantle beneath the Pacific. *J. Geophys. Res.* 102:20395–411

Ritsema J, Ni S, Helmberger DV, Crotwell HP. 1998. Evidence for strong shear velocity reductions and velocity gradients in the lower mantle beneath Africa. *Geophys. Res. Lett.* 25:4245–48

Ritzwoller M, Lavely E. 1995. Three-dimensional seismic models of the Earth's mantle. *Rev. Geophys.* 33:1–66

Robertson GS, Woodhouse JH. 1995. Evidence for proportionality of P and S heterogeneity in the lower mantle. *Geophys. J. Int.* 123:85–116

Robertson GS, Woodhouse JH. 1996. Ratio of relative S to P velocity heterogeneities in the lower mantle. *J. Geophys. Res.* 101:20041–52

Rodgers A, Wahr J. 1993. Inference of core-mantle boundary topography from ISC PcP and PKP travel times. *Geophys. J. Int.* 115:991–1011

Russell S, Lay T, Garnero EJ. 1998. Seismic evidence for small-scale dynamics in the lower most mantle at the root of the Hawaiian hotspot. *Nature* 396:255–58

Russell S, Lay T, Garnero EJ. 1999. Small scale lateral shear velocity and anisotropy heterogeneity near the core-mantle boundary beneath the central Pacific imaged using broadband ScS waves. *J. Geophys. Res.* 104:13181–99

Scherbaum F, Krüger F, Weber M. 1997. Double beam imaging: mapping lower mantle heterogeneities using combinations of source and receiver arrays. *J. Geophys. Res.* 102:507–22

Schimmel M, Paulssen H. 1996. Steeply reflected ScSH precursors from the D″ region. *J. Geophys. Res.* 101:16077–87

Serghiou G, Zerr A, Boehler R. 1998. (Mg,Fe)SiO_3-Perovskite stability under lower mantle conditions. *Science* 280:2093–95

Shearer PM, Hedlin MAH, Earle PS. 1998. PKP and PKKP precursor observations: implications for the small-scale structure of the deep mantle and core. In *The Core-Mantle Boundary*, ed. M Gurnis, ME Wysession, E Knittle, BA Buffett, pp. 37–56. Washington, DC: AGU

Shen Y, Solomon SC, Bjarnason ITh, Wolfe CJ. 1998. Seismic evidence for a lower-mantle origin of the Iceland plume. *Nature* 395:62–65

Sidorin I, Gurnis M. 1998. Geodynamically consistent seismic velocity predictions at the base of the mantle. In *The Core-Mantle Boundary Region*, ed. M Gurnis, M Wysession, E Knittle, B Buffett, pp. 209–30. Washington, DC: AGU

Sidorin I, Gurnis M, Helmberger DV, Ding X-M. 1998. Interpreting D″ seismic structure using synthetic waveforms computed from dynamic models. *Earth Plant. Sci. Lett.* 163:31–41

Song X-D, Helmberger DV. 1997. PKP differential travel times: implications for three-dimensional lower mantle structure. *Geophys. Res. Lett.* 24:1863–66

Souriau A, Poupinet G. 1993. A study of the outermost liquid core using differential travel times of the SKS, SKKS, and S3KS phases. *Phys. Earth Planet. Int.* 68:183–99

Souriau A, Poupinet G. 1994. Lateral variations in P velocity and attenuation in the D″ layer, from diffracted P waves. *Phys. Earth Planet. Int.* 84:227–34

Steinbach V, Yuen DA. 1997. Dynamical effects of a temperature- and pressure-dependent lower-mantle rheology on the interaction of upwelling with the transition zone. *Phys. Earth Planet. Int.* 103:85–100

Steinbach V, Yuen DA. 2000. Viscous heating: a potential mechanism for the formation of the ultra low velocity zone. *Earth Planet. Sci. Lett.* In review

Stixrude L. 1998. Elastic constants and anisotropy of MgSiO3 perovskite, periclase, and SiO2 at high pressure. In *The Core-Mantle Boundary Region*, ed. M Gurnis, M Wysession, E Knittle, B Buffett, p. 83. Washington, DC: AGU

Su W-J, Dziewonski AM. 1991. Predominance of long-wavelength heterogeneity in the mantle. *Nature* 352:121–26

Su W-J, Dziewonski AM. 1992. On the scale of mantle heterogeneity. *Phys. Earth Planet. Int.* 74:29–54

Su W-J, Woodward RL, Dziewonski AM. 1994. Degree 12 model of shear velocity heterogeneity in the mantle. *J. Geophys. Res.* 99:6945–80

Sylvander MS, Ponce B, Souriau A. 1997. Seismic velocities at the core-mantle boundary inferred from P waves diffracted around the core. *Phys. Earth Planet. Int.* 101:189–202

Sylvander MS, Souriau A. 1996a. Mapping S-velocity heterogeneities in the D″ region, from SmKS differential times. *Phys. Earth Planet. Int.* 94:1–21

Sylvander MS, Souriau A. 1996b. P-velocity structure of the core-mantle boundary region inferred from PKP(AB)-PKP(BC) differential travel times. *Geophys. Res. Lett.* 23:853–56

Tackley PJ. 1998. Three-dimensional simulations of mantle convection with a thermochemical basal layer: D″? In *The Core-Mantle Boundary,* ed. M Gurnis, ME Wysession, E Knittle, BA Buffett, pp. 231–53. Washington, DC: AGU

Tackley PJ, Stevenson DJ, Glatzmaier GA, Schubert G. 1993. Effects of an endothermic phase transition at 670 km depth in a spherical model of convection in the Earth's mantle. *Nature* 361:699–704

Tanimoto T. 1990. Long wavelength S-wave velocity structure throughout the mantle. *Geophys. J. Int.* 100:327–36

Thomas C, Weber M, Agnon C, Hofstetter A. 1998. A low-velocity lamellae in D″. *Geophys. Res. Lett.* 25:2885–88

Thomas Ch, Weber M. 1997. P velocity heterogeneities in the lower mantle determined with the German Regional Seismic Network: improvement of previous models and results of 2D modeling. *Phys. Earth Planet. Int.* 101:105–17

Thompson PF, Tackley PJ. 1998. Generation of mega-plumes from the core-mantle boundary in a compressible mantle with temperature-dependent viscosity. *Geophys. Res. Lett.* 25:1999–2002

Valenzuela RW, Wysession ME. 1998. Illuminating the base of the mantle with diffracted waves. In *The Core-Mantle Boundary Region,* ed. M Gurnis, M Wysession, E Knittle, B Buffett, pp. 57–71. Washington, DC: AGU

van der Hilst RD, Kárason H. 1999. Compositional heterogeneity in the bottom 1000 kilometers of Earth's mantle: toward a hybrid convection model. *Science* 283:1885–88

van der Hilst RD, Widiyantoro S, Engdahl ER. 1997. Evidence for deep mantle circulation from global tomography. *Nature* 386:578–84

van der Hilst RD, Widiyantoro S, Creager KC, McSweeney TJ. 1998. Deep subduction and aspherical variations in P-wavespeed at the base of Earth's mantle. In *The Core-Mantle Boundary,* ed. M Gurnis, ME Wysession, E Knittle, BA Buffett, pp. 5–20. Washington, DC: AGU

Vasco DW, Johnson LR. 1998. Whole Earth structure estimated from seismic arrival times. *J. Geophys. Res.* 103:2633–71

Vidael JE. 1987. Waveform effects of a high-velocity, subducted slab. *Geophys. Res. Lett.* 5:542–45

Vidale JE, Benz HM. 1992. A sharp flat section of the core mantle boundary. *Nature* 359:627–29

Vidale JE, Benz HM. 1993. Seismological mapping of fine scale structure near the base of the Earth's mantle. *Nature* 361:529–32

Vidale JE, Hedlin MAH. 1998. Evidence for partial melt at the core-mantle boundary north of Tonga from the strong scattering of seismic waves. *Nature* 391:682–84

Vinnik L, Breger L, Romanowicz B. 1998. Anisotropic structures at the base of the oceanic mantle. *Nature* 393:564–67

Weber M. 1993. P- and S-wave reflections from anomalies in the lowermost mantle. *Geophys. J. Int.* 115:183–210

Weber M. 1994. Lamellae in D″? An alternative model for lower mantle anomalies. *Geophys. Res. Lett.* 21:2531–34

Weber M, Davis JP. 1990. Evidence of a laterally variable mantle structure from P- and S-waves. *Geophys. J. Int.* 102:231–55

Weber M, Davis JP, Thomas Ch, Krüger F, Scherbaum F, et al. 1996. The structure of the lowermost mantle as determined from using seismic arrays. In *Seismic Modeling of Earth Structure,* ed. E Boschi, G Ekstrom, A Morelli, pp. 399–442. New York: North-Holland

Wen L, Helmberger DV. 1998. Ultra-low velocity zones near the core-mantle boundary from broadband PKP precursors. *Science* 279:1701–3

Williams Q. 1998. The temperature contrast across D″. In *The Core-Mantle Boundary,* ed. M Gurnis, ME Wysession, E Knittle, BA Buffett, pp. 73–81. Washington, DC: AGU

Williams Q, Garnero EJ. 1996. Seismic evidence for partial melt at the base of Earth's mantle. *Science* 273:1528–30

Williams Q, Revenaugh JS, Garnero EJ. 1998. A correlation between ultra-low basal velocities in the mantle and hot spots. *Science* 281:546–49

Winchester JP, Creager KC. 1997. High-resolution map of D″ shear-wave velocity anomalies (abstract). *Eos Trans.* Fall Meet. Suppl. AGU. p. 77

Wolfe CJ, Bjarnason ITh, VanDecar JC, Solomon SC. 1997. Seismic structure of the Iceland mantle plume. *Nature* 385:245–47

Woodward RL, Masters G. 1991. Lower-mantle structure from ScS-S differential travel times. *Nature* 352:231–33

Wright C, Lyons JA. 1980. Further evidence for radial velocity anomalies in the lower mantle. *Pageoph.* 119:137–62

Wysession ME. 1996a. Continents of the core. *Nature* 381:373–74

Wysession ME. 1996b. Imaging cold rock at the base of the mantle: the sometimes fate of slabs? In *Subduction: Top to Bottom,* ed. GE Bebout, D Scholl, S Kirby, JP Platt, pp. 369–84. Washington, DC: AGU

Wysession ME. 1996c. Large-scale structure at the core-mantle boundary from diffracted waves. *Nature* 382:244–48

Wysession ME, Bartko L, Wilson JB. 1994. Mapping the lowermost mantle using core-reflected shear waves. *J. Geophys. Res.* 99:13667–84

Wysession ME, Bina CR, Okal EA. 1992. The structure of the core-mantle boundary from diffracted waves. *J. Geophys. Res.* 97:8749–64

Wysession ME, Bina CR, Okal EA. 1993. Constraints on the temperature and composition of the base of the mantle. In *Dynamics of the Earth's Deep Interior and Earth Rotation,* Geophys. Monogr. Ser., ed. J-L LeMouel, et al, pp. 181–90. Washington, DC: AGU

Wysession ME, Fischer KM, Clarke TJ, Al-eqabi GI, Fouch MJ, et al. 1996. Slicing into the Earth. *Eos Trans.* 77:477–80

Wysession ME, Langenhorst A, Fouch MJ, Fischer KM, Al-eqabi GI, et al. 1999. Lateral variations in compressional/shear velocities at the base of the mantle. *Science* 284:120–25

Wysession ME, Lay T, Revenaugh J, Williams Q, Garnero EJ, et al. 1998. The D″ discontinuity and implications. In *The Core-Mantle Boundary,* ed. M Gurnis, ME Wysession, E Knittle, BA Buffett, pp. 273–98. Washington, DC: AGU

Wysession ME, Valenzuela RW, Zhu A-N, Bartko L. 1995. Investigating the base of the mantle using differential travel times. *J. Geophys. Res.* 99:13667–84

Yamada A, Nakanishi I. 1998. Short-wavelength lateral variation of a D″ P-wave reflector beneath the southwestern Pacific. *Geophys. Res. Lett.* 25:4545–48

Young CJ, Lay T. 1987. Evidence for a shear velocity discontinuity in the lower mantle beneath India and the Indian Ocean. *Phys. Earth Planet. Int.* 49:37–53

Young CJ, Lay T. 1989. The core shadow zone boundary and lateral variations of the P velocity structure of the lowermost mantle. *Phys. Earth Planet. Int.* 54:64–81

Zerr A, Boehler R. 1993. Melting of (Mg,Fe)SiO_3-Perovskite to 625 kilobars: indication of a high melting temperature in the lower mantle. *Science* 262:553

Zerr A, Diegeler A, Boehler R. 1998. Solidus of Earth's deep mantle. *Science* 281:243–46